Daily growth-at-risk: financial or real drivers? The answer is not always the same

[Click here to see the latest version]

Helena Chuliá [*] Ignacio Garrón[†] Jorge M. Uribe[‡]

28-02-2023

Abstract

We propose a daily growth-at-risk (GaR) approach, based on high-frequency financial and real indicators, for monitoring downside risks in the US economy. We show that the relative importance of these indicators in terms of their forecasting powers is time varying. Indeed, the optimal forecasting weights of our variables differed clearly between the Global Financial Crisis and the recent Covid-19 crisis, reflecting the dissimilar nature of these two events. We introduce LASSO, elastic net, and adaptive sparse group LASSO into the family of mixed data sampling models used to estimate GaR and show how they outperform previous candidates explored in the literature. Moreover, equity market volatility, credit spreads and the Aruoba-Diebold-Scotti business conditions index are found to be relevant indicators for nowcasting economic activity, especially during episodes of crisis. Overall, our results show that daily information about both real and financial variables is key for producing accurate point and tail risk nowcasts of economic activity.

Keywords: *vulnerable growth, quantiles, machine learning, forecasting, value at risk.*
JEL Classification: *E27, E44, E66.*

[*]Riskcenter- IREA and Department of Econometrics, University of Barcelona, hchulia@ub.edu.
[†]Riskcenter- IREA and Department of Econometrics, University of Barcelona, igarron@ub.edu.
[‡]Faculty of Economics and Business Studies, Open University of Catalonia, juribeg@uoc.edu.

1 Introduction

Many recent studies have analyzed the predictive power of financial variables as indicators of real economic activity in times of crisis. One stream of this literature has emphasized the significant role played by financial indicators in forecasting low quantiles of the real GDP growth rate (e.g., Giglio et al., 2016; Adrian et al., 2019), while another reports that, having controlled for real variables, financial indicators have little to add to the mix (e.g., Reichlin et al., 2020; Plagborg-Møller et al., 2020). And yet, at the same time, a number of studies actually make the opposite claim and conclude that after financial variables have been incorporated into the forecasting equation, real variables have little to add (see Carriero et al., 2022).

This lack of consensus arises because forecasting real economic activity (or any part of the growth distribution, for that matter) using financial variables is a uniquely challenging problem: first, because financial and real variables are generally sampled at different frequencies, the former at a considerably higher frequency than the latter, and, second, because quantifying just how much financial variables add in terms of forecasting power seems to be as much a causal question as a predictive one, inseparable in this regard from the recurring controversy in economics concerning the dichotomy between nominal and real variables, and how (and the extent to which) the former influence the latter. Furthermore, this second concern highlights the tension between what can be considered tasks of pure "prediction" and pure "causal" inference in the social sciences, in general, and in economics, in particular (Athey, 2017). This theoretical distinction is far from clear when it comes to undertaking macroeconomic studies that are, out of necessity, observational and in which forecasting can generally be improved by using domain knowledge that is causal. Moreover, forecasting exercises are generally expected to improve our understanding of the causal mechanisms at work in the economy. In short, we tend to trust forecasts more than we can actually fathom.

Given the complexity of this relationship and the multiplicity of aims that a researcher or policy maker may have when making a forecast, we recommend an eclectic approach be adopted. In so doing, both financial and real variables should ideally be used for forecasting episodes of economic crisis, while the data should be allowed to highlight the relative importance of each set of variables on a time-varying basis. By adhering to such an approach, we are able to make two major contributions to the field. First, we show that the informational content of daily financial and real economy indicators differs across time. Thus, in certain circumstances, forecasting accuracy depends heavily on such financial indicators as the equity market volatility (VXO) index or credit spreads; however, in other circumstances, real economic indicators, such as the Aruoba-Diebold-Scotti business conditions (ADS) index (Aruoba et al., 2009), are better at enhancing forecasts. Here, our results clearly point to the

time-varying importance of real and financial variables. We compute the optimal weights that our nowcasting growth-at-risk (GaR) models assign to the ADS index or to financial variables when combining forecasts and we show that in periods such as the aftermath of the Global Financial Crisis (GFC), financial indicators play a far more relevant role than the ADS index, while the opposite holds true for the recent Covid-19 crisis. This finding is in agreement with the general consensus reached by the macrofinancial literature which highlights the financial nature of the GFC, during which financial markets and intermediaries acted as amplifiers of systemic shocks (Isohätälä et al., 2016; Brunnermeier and Sannikov, 2016; Gertler and Gilchrist, 2018). It is also in agreement with studies claiming that the Covid-19 crisis was simply a product of the supply restrictions imposed to contain the pandemic, which were real and supply-side in nature, albeit with repercussions for aggregate demand (Guerrieri et al., 2022). Thus, it is apparent that understanding the mechanisms underpinning a crisis is a purely causal task that can enable researchers to interpret the results of the forecasting exercise and, to improve the actual forecast.

Second, we also contribute to the GaR literature, as pioneered by Adrian et al. (2019), by using high-frequency financial and real indicators. Unlike most of the literature that employs either quarterly (e.g., Adrian et al., 2019; Brownlees and Souza, 2021) or weekly indicators (Carriero et al., 2022) to forecast tail risk to GDP growth, we estimate our models using daily right-hand side variables. This means our results are based on more real-time information than is usually the case in the extant literature. Exceptions exist - most notably Ferrara et al. (2022) and De Santis and Van der Veken (2020) - however, in the cited instances, real variables are neglected and the number of financial indicators included is limited. Thus, our results are supported by richer cross-sectional information at the intended frequency than is the case in previous studies and so we present models of considerably greater accuracy.

One significant concern that needs to be addressed when working with daily predictors, yet without excluding any variables (financial or real) a priori, is the rate at which the number of parameters to be estimated increases. In this instance, shrinkage, regularization and dimensionality reduction techniques, such as those afforded by LASSO, elastic nets (EN), the adaptive sparse group LASSO or principal components analysis (PCA), become essential. Here, we introduce these methods into mixed data sampling (MIDAS)-Quantile models for estimating GaR and use quantile regression for high-dimensional spaces, as proposed by Belloni and Chernozhukov (2011), and PCA to reduce the dimensions of our problem even further. In line with the warnings reported by Lima et al. (2020) and Lima and Meng (2017), parameterreduction techniques are critical when operating at such high frequencies. The LASSO-Quantile (LASSO-Q) model is described as outperforming other alternatives proposed in the literature, for example, traditional MIDAS quantile regression, where the vector of high-frequency terms takes an arbitrary form, estimated by either frequentist (Ghysels

et al., 2016) or Bayesian methods (Mogliani and Simoni, 2021; Ferrara et al., 2022), both in- and out-of-sample. In addition, in line with Stock and Watson (2004), Andreou et al. (2013), and Ferrara et al. (2022), we show that combined forecasts using all indicators are more accurate, especially out-of-sample.

We validate our conclusions using a battery of statistics drawn from different fields of forecasting and quantitative risk management. Here, rather than relying on a single statistic taken from the forecasting literature which, for instance, may not take into account when the value at risk (VaR) of a series is estimated (low or high conditional quantile), we seek to ensure two properties: unconditional coverage and independence (Christoffersen, 1998). This is important because, as shown by Brownlees and Souza (2021) in a multi-country setting, original indicators of GaR frequently fail to pass basic tests designed in finance to measure the precision of VaR estimates. This, in turn, can call into question the utility of the whole enterprise.

We show that this is not the case for our indicators. In fact, on the vast majority of occasions, daily financial information together with daily information on real activity are especially useful for anticipating adverse scenarios for GDP growth. Moreover, we show that our GaR statistics are adequate and satisfy expectations in terms of performance.

The rest of this paper is organized as follows. Sections 2 and 3 present our data and methodology, respectively. Section 4 presents our main results, while section 5 concludes.

2 Data

Here, we seek to nowcast the conditional tail of the distribution of real GDP growth (or GNP for some of the sample period[1]) on a pseudo real-time basis. To do this, we use the quarterly real-time data set reported by the Federal Reserve Bank of Philadelphia (FRBP) spanning the period from 1986Q1 to 2020Q4. Specifically, this dataset captures the advance estimate for the previous quarter, released towards the end of the month of the current quarter.[2]

In the case of our high-frequency variables, we include 12 daily predictors to make the GaR forecasts (11 financial and 1 real variable). Of this set, eight series are the same as those employed by Pettenuzzo et al. (2016): i) the ADS daily business cycle index designed by Aruoba et al. (2009), which comes from a dynamic factor model at daily frequency; ii) the interest rate spread between the 10-year government bond rate and the federal fund rate (ISPREAD); iii) the change in the effective Federal Funds rate (EFFR); iv) the BAA-AAA-rated corporate bond yield credit spread (CSPREAD); v) the excess return on the market (RET); vi)

[1] In December 1991, the Bureau of Economic Analysis switched from reporting GNP to reporting GDP as its output measure. Later, in January 1996, they also switched from calculating GDP using fixed-weight aggregation to chain-weight methods.

[2] Faust et al. (2013) use this dataset to forecast real-time measures of economic activity using Bayesian model averaging with a large number of real and financial indicators.

the returns on the portfolio of small minus big stocks (SMB); vii) the returns on the portfolio of high minus low book-tomarket ratio stocks (HML); and viii) the returns on a winner minus loser momentum spread portfolio (MOM). In addition, we include four financial indicators: the equity market volatility index (VXO), which has previously been used as a risk indicator;[3] the spread between the yield of 10-year constant maturity Treasury bonds and 3-month Treasury bills (TERM), as a predictor of US recessions;[4] the spread between the 3-month LIBOR based on US dollars and the 3-month Treasury bill spread (TED), as a proxy of credit risk;[5] and the Composite Indicator of Systemic Stress (CISS) for the US, which is a systemic risk measure based on 15 raw market indicators, following a computation analogous to the CISS for the Euro Area (Holló et al., 2012). This last variable is used as a benchmark indicator in our models, as the standard GaR framework considers a composite financial condition index (Adrian et al., 2019; Figueres and Jarociński, 2020). Again, our data sample spans the period from 1986Q1 to 2020Q4 and is restricted by the availability of data for all indicators.

The ADS index is used in our nowcasting exercise with weekly vintages starting 30 November 2008. Although this approach reduces uncertainty at the sample endpoints (Amburgey and McCracken, 2022), uncertainty remains due to the estimation of the ADS index in a previous step. Maldonado and Ruiz (2021) emphasize the importance of measuring this type of uncertainty accurately in empirical applications. This means, for instance, that favourable economic conditions (i.e. better than average) can only be confidently asserted if both the point estimate of the ADS index and its confidence intervals are positive. This uncertainty is, therefore, inherent in our GaR models, given that they use the ADS index as an input variable, and may, as such, produce overstated results (i.e. providing estimates that appear more precise than what they actually are). This limitation applies to all nowcasting exercises that use an index estimated in a prior step (and not only the ADS index), and needs to be acknowledged. We include up to one year of daily lags of the high-frequency indicator in all our specifications. A detailed description of these indicators is provided in Table 1.

[3] Rey (2015) shows that this indicator comoves with global capital flows, global credit growth, and global asset prices. Longstaff et al. (2011) also document that the price of sovereign risk is strongly correlated with VXO.

[4] Estrella and Mishkin (1998) and the subsequent literature have shown the forecasting power of the term spread for recessions.

[5] Gunay (2020) shows that the TED spread is superior to credit default swap indexes as an early warning indicator for the credit market.

Table 1: Detailed description of variables

Variable	Frequency	Sample	Lags	Description	Source
ADS	Daily	Jan. 1, 1986, to Dec. 31, 2020	1 year	ADS index weekly vintages collected in real-time from 30 November 2008	Federal Reserve Bank of Philadelphia
ISPREAD	Daily	Jan. 1, 1986, to Dec. 31, 2020	1 year	Interest rate spread between the 10-year government bond rate and the federal fund rate	Federal Reserve Bank of St. Louis
EFFR	Daily	Jan. 1, 1986, to Dec. 31, 2020	1 year	Effective Federal Funds rate, first difference	Federal Reserve Bank of St. Louis
CSPREAD	Daily	Jan. 1, 1986, to Dec. 31, 2020	1 year	BAA-AAA-rated corporate bond yield credit spread	Federal Reserve Bank of St. Louis
RET	Daily	Jan. 1, 1986, to Dec. 31, 2020	1 year	Excess return on the market, value-weight return of US stocks	Fama and French (1993)
SMB	Daily	Jan. 1, 1986, to Dec. 31, 2020	1 year	The average return on the three small portfolios minus the average return on the three big portfolios	Fama and French (1993)
HML	Daily	Jan. 1, 1986, to Dec. 31, 2020	1 year	The average return on the two value portfolios minus the average return on the two growth portfolios	Fama and French (1993)
MOM	Daily	Jan. 1, 1986, to Dec. 31, 2020	1 year	The average return on the two high prior return portfolios minus the average return on the two low prior return portfolios	Fama and French (1993)
VXO	Daily	Jan. 1, 1986, to Dec. 31, 2020	1 year	Option-based implied volatility measure of S&P100	Federal Reserve Bank of St. Louis
TERM	Daily	Jan. 1, 1986, to Dec. 31, 2020	1 year	Spread between the yield of 10-year constant maturity Treasury bonds and of 3-month Treasury bills	Federal Reserve Bank of St. Louis
TED	Daily	Jan. 1, 1986, to Dec. 31, 2020	1 year	Spread between 3-Month LIBOR based on US dollars and 3-month Treasury bills	Federal Reserve Bank of St. Louis
CISS	Daily	Jan. 1, 1986, to Dec. 31, 2020	1 year	Daily systemic risk measure based on Holló et al. (2012)	European Central Bank
GDP growth	Quarterly	Q1, 1986, to Q4, 2020	1 quarter	Real GDP or Gross National Product, percent change from preceding period, quarterly, seasonally adjusted	Federal Reserve Bank of Philadelphia

3 Methodology

To nowcast tail risks in GDP growth, we extend Adrian et al's (2019) formulation to account for high-frequency (daily) predictors. In this section, we show briefly how we adapt the standard GaR to incorporate daily financial and real indicators using mixed data sampling. To this end, we compare the respective performances of a traditional MIDAS (with Almon lag polynomials), Bayesian MIDAS, LASSO, EN, adaptive sparse group LASSO, and soft and hard thresholding methods. We also show how we combine forecasts, an approach that has been shown to improve forecast accuracy. Finally, we present the tools used to evaluate tail risk forecasts. A quick note for notation: bold letters and symbols refer to multivariate objects such as vectors and matrices.

3.1 Growth-at-risk framework

As in the standard framework of quarterly GaR pioneered by Giglio et al. (2016) and Adrian et al. (2019), we rely on quantile regressions (Koenker and Bassett, 1978). Specifically, we assess the combined effect of past GDP growth (y_{t-h}) and a given financial condition indicator (x_{t-h}) at quarter t and forecast horizon h on current output growth (y_t). At this point it is important to recall that even though x_{t-h} is observed daily, it is aggregated to quarterly frequency by simple averaging.

The baseline quantile regression is given by:

$$y_t = \beta_0(\tau) + \beta_1(\tau) y_{t-h} + \beta_2(\tau) x_{t-h} + \epsilon_t \tag{1}$$

where $\boldsymbol{\beta}(\tau) = (\beta_0(\tau), \beta_1(\tau), \beta_2(\tau))'$ denotes the vector of parameters corresponding to the τ-th quantile, and ϵ_t is a random noise.

The parameters in Eq. (1) are estimated by minimizing the tick loss (TL) function:

$$TL_\tau = \frac{1}{T} \sum_{t=h+1}^{T} \left[\rho_\tau \left(y_t - Q_\tau \left(y_t \mid y_{t-h}, x_{t-h} \right) \right) \right] \tag{2}$$

where $\rho_\tau(\epsilon_t) = (1-\tau)1(\epsilon_t < 0)|\epsilon_t| + \tau 1(\epsilon_t > 0)|\epsilon_t|$, with $1(\epsilon_t < 0)$ taking a value of 1 when the subscript is true and 0 otherwise. The mathematical formulation in Eq. (2) leads to the solution of a linear programming optimization problem that we have not included here. Its basic structure and the counterpart algorithm solution can be found in Koenker (2005).

The predicted value from Eq. (1) is the quantile of $y_{T|T-h}$, which is conditional on the information available up to $T-h$,

$$Q_\tau \left(y_T \mid y_{T-h}, x_{T-h} \right) = \beta_0(\tau) + \beta_1(\tau) y_{t-h} + \beta_2(\tau) x_{t-h}. \tag{3}$$

Koenker and Bassett (1978) further prove that $Q_\tau(y_T | y_{T-h}, x_{T-h})$ is a consistent linear esti-

mator of the conditional quantile function of y_t. In this setting, we are particularly interested in the $GaR(10\%)$ measure defined as the conditional 10% quantile forecast (see, Figueres and Jarociński, 2020; Ferrara et al., 2022; Carriero et al., 2022), namely $Q_{\tau=10\%}(y_T|y_{T-h}, x_{T-h})$.[6]

This last equation can be interpreted as the 10% quantile of GDP growth, which is conditional on the information set available up to $T-h$ for the predictors. On the one hand, a vast literature documents that financial conditions constitute strong predictive information for the lower quantiles of future GDP growth (see, e.g., Adrian et al., 2019; Prasad et al., 2019; Brownlees and Souza, 2021; Figueres and Jarociński, 2020; Ferrara et al., 2022); however, on the other, Plagborg-Møller et al. (2020) and Reichlin et al. (2020) state that controlling for real factors is necessary to measure accurately the real-time effect of financial indicators on real activity. We take these two results into account in the framework we develop here by incorporating, as a high-frequency indicator of the real sector, the Aruoba et al's ADS daily business cycle index (2009), in addition to the financial indicators. We then adopt a combination approach, aimed at producing a better point forecast, and we verify the optimal weights of individual high-frequency predictors by following the literature in this field (see Stock and Watson, 2004; Andreou et al., 2013; Pettenuzzo et al., 2016; Ferrara et al., 2022).

3.2 Adapting the standard GaR approach to high-frequency indicators

The handicap of the formulation as stated in Eq. (1) is that by aggregating the high-frequency indicator, the model cannot respond to daily shocks. Thus, in line with Ferrara et al. (2022), we adapt it so as to account for the daily information flow of the high-frequency indicator up to the latest available observation (minus h_d days), based on the following regression:

$$y_t = \beta_0(\tau) + \beta_1(\tau) y_{t-1} + \boldsymbol{X}^{D\prime}_{t-h_d} \boldsymbol{\phi}(\tau) + \epsilon_t \tag{4}$$

where $\boldsymbol{\phi}(\tau)$ is a $p \times 1$ vector of daily parameters and $\boldsymbol{X}^D_t = \left(x^0_t, x^1_t, \ldots, x^{p-1}_t\right)'$ is a $p \times 1$ vector of the high-frequency variable available on a daily basis, with $x^j_t, j = (0, 1, 2, \ldots, p-1)$, which is updated d times between quarter t and $t-1$. In this setup, we consider y_t as being affected by up to one year ($q = 4$ quarters) of past daily shocks and past GDP growth, giving a total number of parameters (including the constant) approximately equal to $K = q * d + 2 = 4 * 60 + 2 = 242$, assuming a five-day working week ($d = 60$ days); that is, $\boldsymbol{X}^D_{t-h_d} = \left(x^0_t, x^1_{t-\frac{1}{60}}, \ldots, x^{239}_{t-\frac{239}{60}}\right)'$, with $x^j_{t-h_d}$. Notice that in this formulation, the forecast horizon is expressed in high-frequency terms, that is, $h_d = (0, 1/d, 2/d, \ldots, (p-1)/d)$.

Our estimation window is wider than that employed by Ferrara et al. (2022), the latter

[6] Alternatively, Adrian et al. (2019) use the 5% quantile forecast as the measure of tail risk. However, due to our shorter sample period, we opt to use the 10% quantile.

considering a 60-day lag window for the high-frequency indicator. This enables the model to capture up to one year's worth of daily information. In our case, the number of parameters K is relatively higher than the total number of observations T, so we are faced with a parameter proliferation problem, which invalidates the standard estimation procedure of the quantile regression. Thus, in what follows, we discuss the four alternative methods used in our results section to estimate the above regression.

3.3 MIDAS-Q

The MIDAS-Quantile model (MIDAS-Q) offers an effective solution for incorporating highfrequency indicators into Eq. (4), relying on a restriction of the form in which the distributed lags of the high-frequency variable are included in the regression. Specifically, we introduce the high-frequency lagged vector $\boldsymbol{X}^{D}_{t-h_d}$ in a quantile regression for the low-frequency dependent variable y_t as follows:

$$y_t = \beta_0(\tau) + \beta_1(\tau) y_{t-1} + \sum_{j=0}^{p-1} b(j;\boldsymbol{\theta}(\tau)) L^{\frac{j}{d}} x^{j}_{t-h_d} + \epsilon_t \tag{5}$$

where $b(j;\boldsymbol{\theta}(\tau)) = \sum_{i=0}^{c} \theta_{i,j}(\tau) j^i$ is the Almon lag polynomial weighting function, which depends on the vector of parameters $\boldsymbol{\theta}(\tau)$, where $j = (0, 1, 2, \ldots, p-1)$, and the order of the Almon lag polynomial is given by c. While Ghysels et al. (2016) propose the Beta lag polynomial function for the quantile weighting function, we consider the Almon lag polynomial as in other more recent works (Lima et al., 2020; Mogliani and Simoni, 2021; Ferrara et al., 2022). Under the so-called "direct method", Eq. (5) can be reparameterized as follows:

$$y_t = \beta_0(\tau) + \beta_1(\tau) y_{t-1} + \widetilde{\boldsymbol{X}}^{D\prime}_{t-h_d} \boldsymbol{\phi}(\tau) + \epsilon_t \tag{6}$$

where $\widetilde{\boldsymbol{X}}^{D}_{t-h_d} := \boldsymbol{Q} \times \boldsymbol{X}^{D}_{t-h_d}$ is a $(c+1) \times 1$ vector representing the transformed highfrequency predictor, $\boldsymbol{Q}$ is a $((c+1) \times p)$ weighting matrix with the $(i-th+1)$ row element of $\boldsymbol{Q}$ equal to $\left(0^i, 1^i, 2^i, \ldots, (p-1)^i\right)$ for $i = 0, \ldots, c$. Following Ferrara et al. (2022), we set $c = 3$ (third degree Almon lag) and impose two end-point zero restrictions on the slope and the value of the lag polynomial $(r = 2)$, such as $b\left(p-1;\theta_j(\tau)\right) = 0$ and $\nabla_j b\left(j;\theta_j(\tau)\right)\big|_{j=p-1} = 0$, as in Mogliani and Simoni (2021). This causes the weighting structure to slowly reduce to zero. Consequently, the number of parameters of the high-frequency indicator to be estimated is reduced from $(c+1)$ to $(c+1-r)$ parameters.

3.4 BMIDAS-Q

The Bayesian version of the MIDAS-Quantile model (BMIDAS-Q), based on the asymmetric Laplace distribution (ALD) estimation pioneered by Yu and Moyeed (2001), offers a convenient alternative for estimating Eq. (6). This approach is adopted by Ferrara et al.

(2022) to nowcast GaR for the Eurozone when using high-frequency financial indicators. Yu and Moyeed (2001) showed that the minimization problem of quantile regressions (see Eq. (6)) is equivalent to maximizing the likelihood function using the ALD for the error term ϵ_t. Here, we use the Gibbs sampling method as implemented by Kozumi and Kobayashi (2011), alongside their mixture representation of ALD. In this framework, the error term ϵ_t in Eq. (6) can be represented as a location-scale mixture of normal distributions in which the mixing distribution follows an exponential distribution (see Kozumi and Kobayashi, 2011). This implies that Eq. (6) can be expressed as:

$$y_t = \beta_0(\tau) + \beta_1(\tau)y_{t-1} + \widetilde{\boldsymbol{X}}^{D\prime}_{t-h_d}\boldsymbol{\phi}(\tau) + \varphi_1(\tau)v_t + \varphi_2(\tau)\sqrt{\sigma v_t}u_t \tag{7}$$

where φ_1 and φ_2 are fixed parameter functions of the quantile τ, $v_t = \sigma z_t$ follows a standard exponential function, and u_t is a standard normal function. This leads to the following likelihood function (to simplify assume $\boldsymbol{X}_t$ contains all covariates):

$$f\left(y_t \mid \boldsymbol{X}_t'\boldsymbol{\phi}(\tau), v_t, \sigma\right) \propto \exp\left(-\sum_{t=1}^{T}\frac{\left(y_t - \boldsymbol{X}_t'\boldsymbol{\phi}(\tau) - \varphi_1(\tau)v_t\right)^2}{2\varphi_2(\tau)^2\sqrt{\sigma v_t}}\right)\prod_{t=1}^{T}\frac{1}{\sqrt{\sigma v}} \tag{8}$$

with posterior densities for $\boldsymbol{\phi}, v$ and σ given by:

$$\begin{aligned}
\boldsymbol{\phi} \mid \boldsymbol{X}, v, \sigma, \tau &\sim N(\widetilde{\boldsymbol{\beta}}, \widetilde{\boldsymbol{V}}),\\
v \mid \boldsymbol{X}, \boldsymbol{\phi}, \sigma, \tau &\sim GiG\left(\frac{1}{2}, \frac{\left(y_t - \boldsymbol{X}_t'\boldsymbol{\phi}(\tau)\right)^2}{\sigma\varphi_2(\tau)^2}, \frac{2}{\sigma} + \frac{\varphi_1(\tau)^2}{\sigma\varphi_2(\tau)}\right),\\
\sigma \mid \boldsymbol{X}, v, \boldsymbol{\phi}, \tau &\sim \text{Inv-Gamma}(a, b),
\end{aligned}$$

where

$$\widetilde{\boldsymbol{\beta}} = \widetilde{\boldsymbol{V}}\left(\sum_{t=1}^{T}\frac{\boldsymbol{X}_t\left(y_t - \varphi_1(\tau)v_t\right)}{\varphi_2(\tau)^2\sigma v_t}\right) \text{ and } \widetilde{\boldsymbol{V}}^{-1} = \sum_{t=1}^{T}\frac{\boldsymbol{X}_t'\boldsymbol{X}_t}{\varphi_2(\tau)^2\sigma v_t} + \widetilde{\boldsymbol{V}}_0^{-1}$$

and a and b are shape and scale parameters of the inverse gamma distribution, respectively. In our framework, as in that employed by Carriero et al. (2022), we are interested in using the posterior mean of the coefficient vector $\boldsymbol{\phi}(\tau)$ to produce point forecasts.

3.5 Soft thresholding: LASSO-Q and EN-Quantile (EN-Q)

One caveat of the restricted MIDAS approach presented above is that the predetermined choice of the weighting function might result in a lag structure for the high-frequency predictor that fails to maximize forecast accuracy. Thus, as an alternative, we propose estimating GaR by using either the LASSO or EN regularization for choosing a lag structure for the high-frequency predictors (Bai and Ng, 2008; Lima et al., 2020).

Accordingly, we select the lags of the high-frequency variable, based on the LASSO-Q algorithm proposed by Belloni and Chernozhukov (2011). The model can be summarized as follows,

$$\min_{\beta,\phi} E[\rho_\tau(y_t - \beta_0(\tau) - \beta_1(\tau)y_{t-1} - \boldsymbol{X}^{D'}_{t-\mathrm{h}_d}\boldsymbol{\phi}(\tau))] + \lambda_\tau[\frac{\sqrt{\tau}(1-\tau)}{T}]\sum_{j=0}^{p-1}|\phi_j(\tau)| \tag{9}$$

where the optimization problem is the sum of the standard quantile minimization function (as in Eq. (2)) and a penalty function given by a scaled l_1-norm of the daily vector of parameters $\phi_j(\tau)$. The overall penalty is given by $\lambda_\tau[\sqrt{\tau(1-\tau)}/T]$, where T is the sample size. The optimal level of λ_τ (LASSO-Q penalization) is calculated as in Belloni and Chernozhukov (2011). The LASSO-Q penalty has the distinctive feature of making the coefficients of insignificant predictors exactly equal to zero, retaining only the informative predictors for the forecast.

The Zou and Hastie's (2005) EN estimator seeks to address two potential drawbacks of the original LASSO. First, if $K > T$, LASSO can select T variables at most. Second, if there is a group of variables with high pairwise correlation coefficients, LASSO tends to select only one variable from the group and does not care which one. Both, LASSO and EN shrink the estimates and perform model selection. However, while the LASSO penalty is convex, the EN penalty is strictly convex, which means that predictors must be grouped to have similar coefficients. The EN-Q objective function is given by:

$$\min_{\beta,\phi} E\left[\rho_\tau\left(y_t - \beta_0(\tau) - \beta_1(\tau)y_{t-1} - \boldsymbol{X}^{D'}_{t-\mathrm{h}_d}\boldsymbol{\phi}(\tau)\right)\right] + \lambda_{1,\tau}\sum_{j=0}^{p-1}\left|\phi_j(\tau)\right| + \lambda_{2,\tau}\sum_{j=0}^{p-1}\phi_j(\tau)^2 \tag{10}$$

where $\lambda_{1,\tau}$ and $\lambda_{2,\tau}$ are two tuning parameters that satisfy $\frac{\lambda_{2,\tau}}{\lambda_{1,\tau}+\lambda_{2,\tau}} > 0$. This restriction implies that the EN-Q is strictly convex, so it forces high pairwise correlated predictors to have similar coefficients. As a result, EN-Q stretches the net so as to retain all the important predictors, even if they are highly correlated.

As Zou and Hastie (2005) show, the EN objective function can be reformulated as a LASSO problem.[7] This has appealing computational properties, since we can use the Belloni and

[7] Bai and Ng (2008) and Lima et al. (2020) use this approach to produce conditional mean forecasts with different loss functions. The former apply the mean square error and the latter the TL function.

Chernozhukov (2011) algorithm to estimate the EN-Q model. To implement this, let's first define (where for the sake of simplicity, we assume that $\boldsymbol{X}_t$ contains all the covariates): $y_t^+(\tau) = \left(y_t \boldsymbol{O}_p\right)'$ and $\boldsymbol{X}_t^+(\tau) = \frac{1}{\sqrt{1+\lambda_{2,\tau}}}\left(\boldsymbol{X}_t \sqrt{\lambda_{2,\tau}} \boldsymbol{I}_p\right)'$, where $\boldsymbol{O}_p$ represents a $p \times 1$ vector of zeros and $\boldsymbol{I}_p$ is a $p \times p$ identity matrix.

Based on this new formulation, Eq. (10) can be re-expressed as follows,

$$\min_{\boldsymbol{\phi}^{++}} E\left[\rho_\tau\left(y_t^+ - \boldsymbol{X}_t^{+\prime}\boldsymbol{\phi}(\tau)\right)\right] + \gamma_\tau \sum_{j=0}^{p-1} \left|\phi_j(\tau)\right| \tag{11}$$

where $\gamma_\tau = \frac{\lambda_{1,\tau}}{\sqrt{1+\lambda_{2,\tau}}}$. Notice that now the sample size is equal to $T + p$, which enables EN to select all p high-frequency predictors in all cases. To remove the double shrinkage effect from LASSO, the EN-Q estimator is $\boldsymbol{\phi}^+(\tau) = (1 + \lambda_{2.\tau})\,\boldsymbol{\phi}^{++}(\tau)$ (see Zou and Hastie, 2005). In our application, we only apply this correction if we use the EN-Q model to produce the conditional quantile nowcasts directly.

3.6 Soft and hard thresholding methods: LASSO-PCA-Q and EN-PCA-Q

In line with Lima et al. (2020) and Bai and Ng (2008), we apply soft and hard thresholding methods when making forecasts with many predictors. To implement this approach, we estimate principal components from the non-zero coefficients selected by LASSO-Q or EN-Q and, using these selected variables, we can estimate factors by PCA and select the optimal number of factors using the eigen ratio (Ahn and Horenstein, 2013). Finally, we retain the factors associated with p-values lower than 0.01 (or the statistically most significant). To differentiate these models from those that only use the soft threshold to make their forecasts (i.e. LASSO-Q and EN-Q), we label models of this type as LASSO-PCA-Q and EN-PCA-Q, with the first step being selected by LASSO-Q or EN-Q, respectively.

3.7 Adaptive sparse group LASSO (ASGL-Q)

In line with Mendez-Civieta et al. (2021), we introduce a novel framework based on an adaptive sparse group LASSO-Quantile (ASGL-Q) regression framework [8]. This technique is particularly suited to high-dimensional problems where $(p >> T)$ and, therefore, for dealing with multiple groups of high-frequency variables, with sparsity allowed within the high-frequency lagged vector. It also uses adaptive weights in the penalization scheme, in line with Zou (2006). For simplicity of notation, we refer to $TL_\tau(\boldsymbol{\phi}(\tau))$ as the TL function of the vector of parameter $\boldsymbol{\phi}(\tau)$ (see Eq. (2)).

[8] We thank an anonymous reviewer for suggesting this model.

The ASGL-Q objective function is given by:

$$\min_{\phi} E\left[TL_{\tau}(\boldsymbol{\phi}(\tau)) + \alpha\lambda \sum_{j=0}^{p-1} \widetilde{w}_j \left|\phi_j(\tau)\right| + (1-\alpha)\lambda \sum_{l=0}^{m-1} \sqrt{p_l}\tilde{v}_l \left\|\phi(\tau)^l\right\|_2\right] \tag{12}$$

where $\widetilde{w}_j$ is the weight of the $j-th$ parameter $\phi_j(\tau)$, $\tilde{v}_l$ is the weight of the $l-th$ group of parameters (or high-frequency variable) $\phi(\tau)^l$, and p_l is the size of the $l-th$ group. Overall, these weights assign a low weight to a relatively important high-frequency variable (or to a given lag) and thus penalize less. Notice that Eq. (12) is a linear combination of LASSO and group LASSO, given by λ and the tradeoff between them, $\alpha \in [0,1]$. Specifically, a value close to 1 leads to the additive LASSO while a value close to 0 leads to the additive sparse group LASSO. Thus, this formulation provides solutions that are both between and within groups. Also, as pointed out by Mendez-Civieta et al. (2021), this formulation defines a convex function which ensures that the solution of the minimization process is a global minimum.

3.8 Forecast Combination

An extensive literature reports the superior performance of forecast combinations, reflecting the fact that they draw on information from all the underlying models as opposed to relying on just one specific model (e.g., Stock and Watson, 2004; Andreou et al., 2013; Pettenuzzo et al., 2016; Ferrara et al., 2022). Indeed, selecting just one model can be both inconvenient and misleading in the presence of a misspecification (Hansen et al., 2011). While different methods have been developed for implementing forecast combinations, here we opt for the discounted meansquared forecast error combination approach (Stock and Watson, 2004; Andreou et al., 2013), using the TL as the objective function.

Combination weights are computed recursively on a daily basis as follows:

$$\begin{aligned} w_{i,t-h_d} &= \frac{\lambda_{i,t-h_d}^{-\kappa}}{\sum_i^N \lambda_{i,t-h_d}^{-\kappa}}, \\ \lambda_{i,t-h_d} &= \sum_{s=T_o}^{T_f} \delta^{T_f-s} \left(y_s - GaR_{i,s}(10\%)\right) \times \left(\tau - 1(y_s < GaR_{i,s}(10\%))\right), \end{aligned} \tag{13}$$

where $w_{i,t-h_d}$ is the weight corresponding to the individual $GaR_{i,s}(10\%)$ measure based on the high-frequency indicator i, which depends on the discounted TL given by $\lambda_{i,t-h_d}$, with discount factor $\delta = 0.9$ and $\kappa = 1$. Importantly, $s = T_o$ is the point at which the first prediction is computed, and $s = T_f$ is the point at which the most recent prediction can be evaluated with the high-frequency indicator up to the latest available observation. By using

this framework, we can compute a combined GaR(10%) for each model.

3.9 GaR evaluation

We evaluate tail risk forecasts using a battery of indicators developed in the forecast and risk management literatures. Our main tool for assessing $GaR(10\%)$ point forecasts is the average TL, which has been shown to be particularly appropriate when the object of interest is the forecast of a certain quantile of the dependent variable's conditional distribution (see Giacomini and Komunjer, 2005; Gneiting and Raftery, 2007; Gneiting and Ranjan, 2011; Manzan, 2015). Carriero et al. (2022) specifically use this loss function to evaluate the predictive capacity of their models for quantifying tail risks.

The average TL for $\tau = 0.10$ is specified as follows,

$$TL_{\tau=10\%} = \frac{1}{T}\sum_{t=1}^{T}\left(y_t - GaR_t(10\%)\right) \times \left(\tau - 1(y_t < GaR_t(10\%))\right), \tag{14}$$

where y_t is the actual GDP growth, $GaR_t(10\%)$ is the 10% predictive quantile of GDP growth, and the indicator function $1(y_t < GaR_t(10\%))$ takes a value of 1 if it is below the 10% forecast quantile and 0 otherwise. Following convention (see Corradi and Swanson, 2006; Clark and McCracken, 2013), we use the Diebold and Mariano (1995) test[9] to assess the relative forecasting accuracy of our GaR models. In all instances, the models compared are non-nested. In the recent literature, Andreou et al. (2013), Pettenuzzo et al. (2016), and Carriero et al. (2022) have adopted the same approach.

In addition, we employ two coverage tests commonly used in the risk management literature to assess interval forecasts. In line with Christoffersen (1998), the problem of assessing the adequacy of a VaR model can be reduced to the problem of determining whether the indicator of excess sequence (i.e. the $1(y_t < GaR_t(10\%))$) has two properties: i) an unconditional coverage property, and ii) an independence property. In this setting, GaR forecasts are evaluated using the TL, a loss function generally used to assess the accuracy of VaR predictions (Giacomini and Komunjer, 2005). We evaluate these two conditions using the unconditional coverage (UC), and the dynamic quantile (DQ) tests (Engle and Manganelli, 2004), respectively. Specifically, the DQ is estimated using four lags of the excess sequence indicator (see Engle and Manganelli, 2004). Brownlees and Souza (2021) follow a similar approach for a multi-country GaR evaluation. Note that these two conditions can be achieved by more than one model; thus, ultimately, the TL is used in the final selection of the best performing model.

[9] We use the variance adjustment proposed by Harvey et al. (1997), which is supported by the results in Clark and McCracken (2013).

4 Empirical analysis

This section presents the statistical details for the computation of each model and the outcomes of the nowcasting exercise.

4.1 Parameterization and computational approach

We consider different high-frequency GaR measures covering different variables and models. Below we discuss our choice of parameters for each model:

- MIDAS-Q: Eq. (6) is estimated by adopting the quantile approach described in Section 3.3, in which we consider a third degree Almon lag polynomial $(c = 3)$ with two endpoint restrictions $(r = 2)$, so that the number of parameters of the high-frequency indicator is reduced substantially to $c + 1 - r$. This lag structure presents good economic properties as it slowly decays towards zero (see Mogliani and Simoni, 2021).

- BMIDAS-Q: Based on the aforementioned constrained Almon lag structure for the high-frequency variable, Eq. (7) is estimated using the Bayesian methodology considered in Section 3.4. Specifically, the model considers standard uninformative priors on the coefficient vector to have a mean equal to 0 and a variance where all elements in the diagonal are equal to 9, except for the autoregressive lag of GDP, whose prior mean and variance are set at 0.5 and 0.1, respectively. Also, the scale and shape parameters of the inverse gamma function are set at 0.01. The Gibbs sampler is used to estimate the model parameters with 10,000 repetitions (for computational efficiency), after a burn-in period of 1,000 iterations, using the normal approximation, which simplifies the algorithm (Yang et al., 2015).[10] The choice of these parameters closely resembles those made by Ferrara et al. (2022), which constitutes a natural benchmark model for our work.

- LASSO-Q: In line with the model presented in Section 3.5, we set the penalty parameter λ equal to the 0.9 quantile of the pivotal distribution (see Belloni and Chernozhukov, 2011). Figure A1 shows the selected lags for LASSO-Q using each highfrequency predictor. Interestingly, historically it not only tends to select the most recent daily lag of the given quarter (as one would expect), but others from past quarters. This is a key difference of this technique when compared to MIDAS-Q and BMIDAS-Q, as the latter models have an arbitrary decaying weighting scheme.

- EN-Q: Based on the model presented in Section 3.5, $\lambda_{1,\tau}$ is set as the penalty parameter of the LASSO-Q model, defined as above, and $\lambda_{2,\tau}$ is obtained by minimizing the mean cross-validated errors of the model, with the EN mixing parameter set at $\alpha = 0.5$

[10] See Kozumi and Kobayashi (2011) for details on the estimation procedure.

(Friedman et al., 2010). Figure A2 shows the selected lags for EN-Q using each high-frequency predictor. Analogous to LASSO-Q, we observe that this model historically selects different daily lags for each high-frequency variable.

- LASSO-PCA-Q and EN-PCA-Q: Based on the non-zero high-frequency lags selected with either LASSO-Q or EN-Q, we estimate factors by PCA, select the optimal number of factors using the eigen ratio (Ahn and Horenstein, 2013), and retain the factors associated with p-values lower than 0.01 (or the statistically most significant). The final step in this procedure is estimated using the quantile approach described in Section 3.1.

- ASGL-Q: Based on the model presented in Section 3.7, we consider the following parametrization procedure. First, we carry out cross-validation checks for different values of λ and α to obtain their optimal values. By estimating this model with the full sample and all the high-frequency variables (except the CISS, which is used as a benchmark), we obtain the optimal values of $\lambda = 0.010$ and $\alpha = 0.25$, which minimize the TL function. Second, we compute recursively both LASSO weights and group LASSO weights based on the regression on a subset of principal components. As suggested by Mendez-Civieta et al. (2021), this method achieves better results in terms of prediction error and the stability of the variables selected when used in real datasets.

For each of these models,[11] we construct the individual $GaR(10\%)$ nowcasts by estimating the 10% quantile forecast $\widehat{Q}_{\tau=10}\% \left(y_T \mid y_{T-1}, \boldsymbol{X}^D_{i,T-h_d} \right)$ conditional on one lag of GDP growth and the respective high-frequency indicator, as described in Table 1. This measure is computed recursively on a daily basis for each specification including a high-frequency indicator $\boldsymbol{X}^D_{i,T-h_d}$. The estimation sample spans the period from 1986Q1 to 2020Q4, and the daily nowcasts start on January 1, 2007.

$$GaR^*_T(10\%) = \sum_i w_{i,T-h_d} \times \widehat{Q}_{\tau=10\%} \left(y_T \mid y_{T-1}, \boldsymbol{X}^D_{i,T-h_d} \right) \tag{15}$$

Eq. (15) allows us to capture the relative importance of individual $GaR(10\%)$ estimates and to deal with the potential problem of introducing many, potentially correlated, series into a common framework. It should again be stressed that the combined $GaR(10\%)$ does not include the CISS, as it is the benchmark financial composite indicator. Figure A3 provides a recursive plot of the combination weights assigned to the various models using the forecast combination approach. We find that both high-frequency real and financial indicators are important in providing accurate GaR(10%) nowcasts and that the importance of each is time varying.

[11] In the case of the AGSL-Q model, since it allows for multiple groups of variables, we compute the conditional 10% quantile using all the high-frequency indicators (except the CISS, which is the benchmark); thus, it directly produces a combined GaR forecast.

4.2 Nowcasting GaR

We recursively estimate all the specifications identified above for each quarter spanning the period from 1986Q1 to 2006Q4 and construct daily GaR nowcasts in pseudo real-time as of 1 January 2007.

We begin by showing the combined GaR(10%) forecasts made by our LASSOQ model[12] and compare these to two alternative specifications, the individual GaR(10%) using the CISS and the combined GaR(10%) estimated by ASGL-Q. Recall that while LASSO-Q combines forecasts as explained in Section 4.1, ASGL-Q uses all the information directly in the estimation. Figure 1a shows the preliminary real-time estimates of quarterly US growth rate along with the combined GaR(10%) and the two alternative models. Overall, it is evident that the large negative growth rates recorded during periods of recession, such as the GFC in 2008-2009 and the Covid-19 pandemic (that started in 2020), are captured effectively by our combined GaR(10%), while this is not the case for the second event when using the alternative specifications. First, the difference in predictive powers between LASSO-Q and ASGL-Q is due in part to the difference in their combination schemes (see Figures 1b and 1c); thus, while the weights of the former are more volatile, those of the latter are more stable. Interestingly, in both frameworks, at the onset of the Covid-19 pandemic a larger weight is assigned to the ADS indicator, highlighting the benefits of using real indicators in a GaR framework. Second, relative to the individual GaR using the CISS and the standard GaR framework that uses only a composite financial condition index (Adrian et al., 2019), an evident strength of our framework is that it permits the use of a wider range of indicators which improves the accuracy of our predictions. Figure 1b provides a clearer indication of this by presenting the daily combination weights assigned to the different individual GaR nowcasts. Here, it is apparent that the relative importance of real and financial indicators is time varying. In the case of the 2008 GFC, the ADS, VXO and CSPREAD indicators receive a relatively high weight across all models; in contrast, on the onset of the Covid-19 pandemic, all the models assign higher weights to the ADS. This first result is in line with the general consensus in the macro-financial literature stressing the financial nature of the GFC, in which both financial intermediaries and financial markets amplified the shocks to the real economy (Isohätälä et al., 2016; Brunnermeier and Sannikov, 2016; Gertler and Gilchrist, 2018). However, the second result indicates that the Covid-19 crisis was a product of the supply restrictions imposed to contain the pandemic, which were real and supply-side in nature (Guerrieri et al., 2022). Consequently, our optimal estimated weights suggest that it is fundamental to include both real and financial daily indicators to improve GaR nowcasts. Interestingly, the closely related

[12] We opt to report here the combined GaR nowcasts of the LASSO-Q model as, in general, it performs relatively well in terms of the average TL function compared to the rest of the models (see Table 2). The results for the other models are available upon request.

studies conducted by Ferrara et al. (2022) and De Santis and Van der Veken (2020), which only include daily financial variables in the GaR framework, fail to capture the real magnitude of the risks during the Covid-19 epidemic. This indicates that financial variables alone play only a modest role in gauging the effect of this last recession.

Figure 1: GaR results for LASSO-Q and ASGL-Q

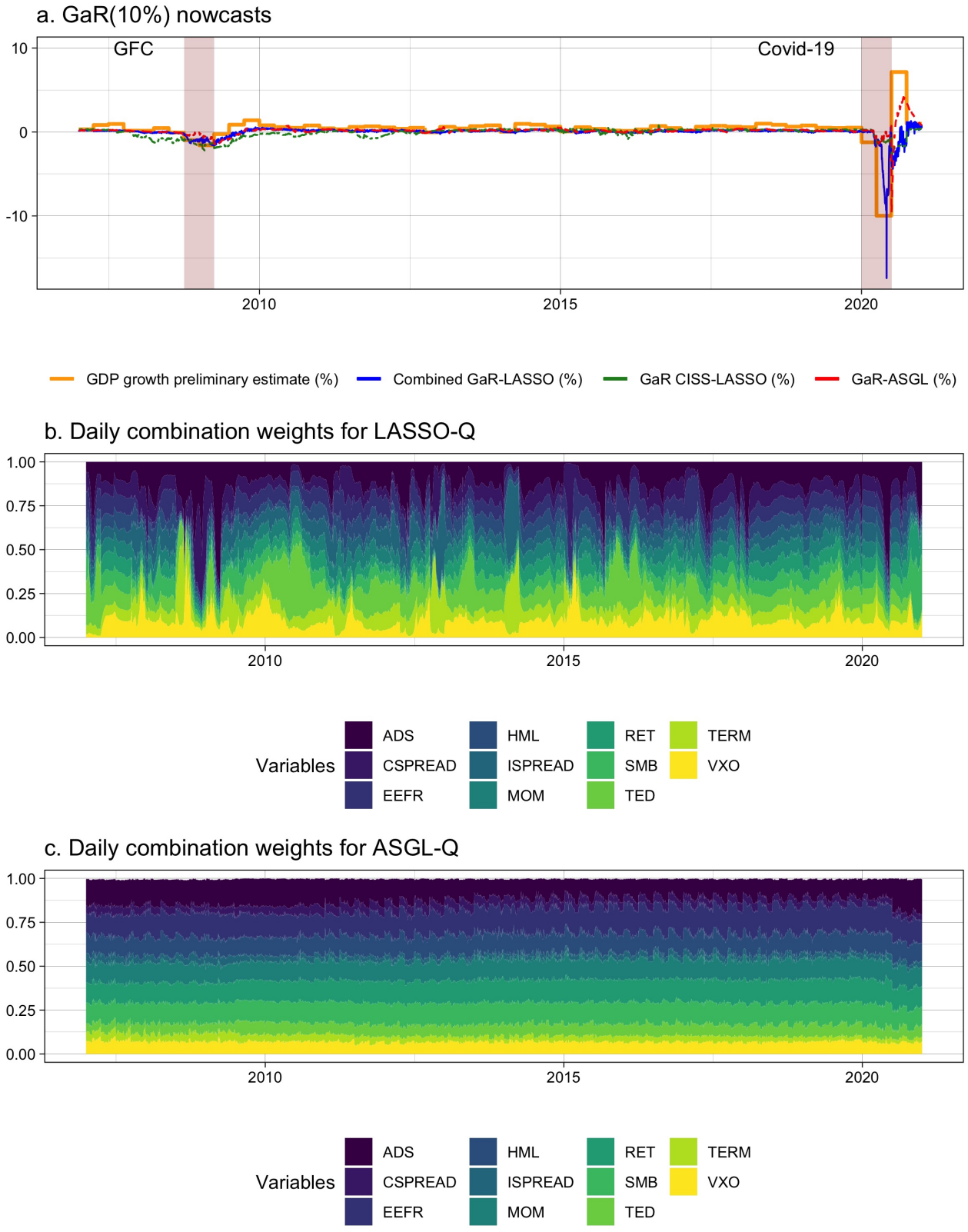

Note: The estimation sample spans the period from 1986Q1 to 2020Q4, and the daily nowcasts start as of 1 January 2007. In Panel a, the area shaded red represents NBER recessions at the end of the period. In Panel c, we omit the weight of the lagged GDP growth as it is close to zero.

4.3 Evaluation

In this section we assess the relative performance of *i*) combined GaR nowcasts based on real and financial indicators vs. individual GaR nowcasts using a financial condition index (i.e. CISS) as a benchmark; and *ii*) individual GaR nowcasts of financial and real indicators vs. the combined GaR nowcasts, in line with Figueres and Jarociński (2020).

4.3.1 Combined GaR (using financial and real variables) vs. standard GaR

Table 2 reports the relative average TL function of a given combined GaR model compared to that of the benchmark model (an individual GaR using the CISS), together with their DM test statistic values. A TL value lower than one implies that the combined model outperforms the benchmark, while in the case of the DM test the alternative hypothesis is that the indicated forecast is more accurate than that of the benchmark (i.e. rejection of the null is our preferred outcome). Notably, most models outperform the benchmark and so we can reject the hypothesis of equality of forecasts according to the DM test with a 10% confidence level. This provides strong evidence of the benefits of combining multiple real and financial indicators within the GaR framework. Interestingly, the LASSO-Q model tends to provide a lower average TL function and often rejects the null hypothesis of the DM test for different daily horizons, for both periods (that is, before and after the Covid-19). We provide evidence that the LASSO lag selection improves forecast accuracy while imposing fewer restrictions than those imposed by traditional MIDAS models.

Table 3 reports the tests commonly used in the financial risk management literature, namely the UC and the DQ tests, to assess interval forecasts for the combined GaR models. Specifically, the UC tests the probability of the null hypothesis that the proportion of exceedances is equal to the quantile (non-rejection is our preferred outcome), while the DQ tests the probability of the null hypothesis that the exceedance indicator is an i.i.d. process (non-rejection is again our preferred outcome). Overall, models using LASSO or EN perform better than MIDAS on these adequacy tests, with a higher number of non-rejections at the 10% level of probability. These results hold for both the period before Covid-19 and the period including it.

4.3.2 Combined GaR (using financial and real variables) vs. individual GaR

Next, we address the question as to whether combined or individual indicators provide more accurate nowcasts, also building on Figueres and Jarociński (2020). Table 4 reports the relative average TL function of an individual GaR vs. that of the combined GaR (benchmark) using LASSO-Q, together with their DM test statistic values. Again, a TL value lower than one implies that the individual GaR outperforms the benchmark (the combined GaR), while in the case of the DM test the alternative hypothesis is that the indicated forecast is more accurate than the benchmark. In this setting, we would prefer to obtain a TL with a value greater

Table 2: Out-of-sample forecast accuracy based on the relative TL

	$h_d = 0$		$h_d = 10$		$h_d = 20$		$h_d = 40$		$h_d = 60$	
	TL	DM	TL	DM	TL	DM	TL	DM	TL	DM
Panel A. Before COVID-19 (2007Q1 to 2019Q4)										
GaR^{MIDAS}	0.641	**0.001**	0.655	**0.001**	0.653	**0.000**	0.686	**0.001**	0.683	**0.001**
GaR^{BMIDAS}	0.606	**0.000**	0.616	**0.000**	0.631	**0.001**	0.643	**0.001**	0.654	**0.001**
GaR^{LASSO}	0.590	**0.001**	0.559	**0.000**	0.569	**0.000**	0.769	0.145	0.843	0.232
GaR^{EN}	0.956	0.415	0.978	0.461	0.932	0.366	0.853	0.273	0.858	0.277
$GaR^{LASSO-PCA}$	0.617	**0.001**	0.638	**0.002**	0.706	**0.010**	0.830	0.225	0.857	0.266
GaR^{EN-PCA}	0.617	**0.001**	0.691	**0.010**	0.741	**0.039**	0.809	0.176	0.844	0.251
GaR^{ASGL}	1.102	0.646	1.037	0.559	0.983	0.471	0.945	0.419	1.221	0.744
Panel B. Including COVID-19 (2007Q1 to 2020Q4)										
GaR^{MIDAS}	0.855	**0.027**	0.82	**0.005**	0.804	**0.022**	0.558	**0.094**	0.943	0.201
GaR^{BMIDAS}	0.878	**0.021**	0.849	**0.000**	0.839	**0.005**	0.558	**0.087**	0.932	0.141
GaR^{LASSO}	0.864	**0.002**	0.773	**0.006**	0.458	**0.096**	0.501	0.121	0.895	**0.092**
GaR^{EN}	0.953	0.243	0.969	0.330	0.822	0.153	0.563	0.139	0.917	0.173
$GaR^{LASSO-PCA}$	0.940	0.263	0.733	**0.041**	0.488	0.116	0.593	0.133	0.927	0.120
GaR^{EN-PCA}	0.911	0.102	0.850	**0.013**	0.841	**0.064**	0.691	0.116	0.903	0.123
GaR^{ASGL}	1.106	0.790	1.002	0.506	1.027	0.614	1.056	0.687	1.085	0.766

Note: This table shows the TL for each combined GaR relative to the individual GaR considering the CISS, for different daily horizons. We also report the p-values of the DM test for the null hypothesis of equality of forecasts, conducted on a one-sided basis, such that the alternative hypothesis is that the indicated forecast is more accurate than the benchmark (a rejection of the null is preferred). If the p-value is below 0.10 (bold values), we conclude that the forecast from a combined GaR model is more accurate than that of the benchmark.

than 1 and, thus, not reject the null hypothesis, in order to have evidence of the greater accuracy of our combined GaR framework. Overall, our results suggest that we cannot reject the null hypothesis of the DM test with a 10% confidence level, indicating that our combined GaR is indeed more accurate. However, the individual GaR specification using the ADS indicator is the only model to present a relative TL value lower than one for daily horizons greater or equal to 10 days and for the period including the Covid-19 pandemic. This suggests, in line with Pettenuzzo et al. (2016) and Lima et al. (2020), that individual GaR models that include the ADS index perform relatively better than their counterparts that do not include it. Moreover, this result recognizes that the Covid-19 crisis was a product of the supply restrictions imposed to contain the pandemic, which were real and supply-side in nature (Guerrieri et al., 2022). Results for alternative models are presented in Appendix B.

Table 5 reports the UC and the DQ test results when assessing interval forecasts for the different individual GaR specifications estimated by LASSO-Q. Again, the UC tests the prob-

Table 3: Out-of-sample forecast accuracy based on coverage tests

	$h_d = 0$		$h_d = 10$		$h_d = 20$		$h_d = 40$		$h_d = 60$	
	UC	DQ	UC	DQ	UC	DQ	UC	DQ	UC	DQ
Panel A. Before COVID-19 (2007Q1 to 2019Q4)										
GaR^{MIDAS}	0.001	**0.619**	0.019	**0.164**	0.019	**0.144**	0.019	**0.141**	0.001	**0.619**
GaR^{BMIDAS}	0.001	**0.619**	0.001	**0.619**	0.001	**0.619**	0.001	**0.619**	0.001	**0.619**
GaR^{LASSO}	0.019	**0.849**	**0.273**	0.014	**0.273**	0.018	0.095	**0.590**	0.019	**0.272**
GaR^{EN}	**0.273**	**0.180**	**0.273**	**0.218**	**0.926**	**0.126**	**0.273**	0.045	**0.273**	**0.107**
$GaR^{LASSO-PCA}$	0.095	**0.316**	0.095	**0.344**	**0.273**	**0.378**	0.095	**0.630**	0.095	0.011
GaR^{EN-PCA}	0.019	**0.842**	**0.565**	0.021	**0.273**	**0.386**	0.095	**0.603**	0.095	**0.631**
GaR^{ASGL}	**0.427**	0.013	**0.226**	0.071	**0.226**	0.044	**0.926**	**0.200**	**0.226**	**0.493**
Panel B. Including COVID-19 (2007Q1 to 2020Q4)										
GaR^{MIDAS}	**0.208**	0.001	**0.455**	0.045	**0.455**	0.085	**0.455**	0.024	**0.208**	0.003
GaR^{BMIDAS}	0.068	0.040	0.068	0.063	0.068	0.080	0.068	0.080	0.068	0.080
GaR^{LASSO}	0.068	**0.917**	**0.786**	0.000	**0.786**	0.021	**0.786**	0.042	**0.208**	**0.266**
GaR^{EN}	**0.786**	0.007	**0.786**	0.009	**0.547**	0.029	**0.786**	0.042	**0.786**	0.076
$GaR^{LASSO-PCA}$	**0.455**	**0.235**	**0.455**	0.009	**0.786**	0.036	**0.455**	**0.118**	**0.455**	0.008
GaR^{EN-PCA}	**0.208**	**0.468**	**0.547**	0.000	**0.860**	**0.202**	**0.455**	**0.130**	**0.455**	**0.677**
GaR^{ASGL}	**0.160**	0.015	0.031	0.000	0.031	0.000	**0.312**	**0.237**	**0.031**	**0.371**

Note: This table shows the following two interval tests for different combined GaR models: Kupiec's (1995) unconditional coverage test (UC), where the null hypothesis is that the proportion of exceedances is equal to the quantile (non-rejection of the null is preferred); and the dynamic quantile test (DQ) of Engle and Manganelli (2004), where the null hypothesis is that the exceedance indicator is an i.i.d. process (non-rejection of the null is preferred). Bold values indicate that model passes the test with a 10% level of probability.

ability that the proportion of exceedances is equal to the quantile (where non-rejection of the null is our preferred outcome) and the DQ tests the probability that the exceedance indicator is an i.i.d. process (where non-rejection of the null is again our preferred outcome). For individual GaR specifications the evidence is mixed, depending on the daily horizon. Results for alternative models are presented in Appendix C.

Overall, the evidence we present here supports the time-varying importance of both daily financial and real indicators for estimating GaR. Our results are consistent with those for the eurozone reported by Ferrara et al. (2022) and for the US reported by De Santis and Van der Veken (2020), insofar as daily financial variables provide policymakers with timely warnings about the downside risks of GDP. Nevertheless, we are able to provide further and clearer evidence, in line with the suggestions made by Pettenuzzo et al. (2016), that stress the benefits of incorporating a high-frequency real indicator, such as the ADS index, in the forecasting

Table 4: LASSO-Q out-of-sample forecast accuracy based on the relative TL

	$h_d = 0$		$h_d = 10$		$h_d = 20$		$h_d = 40$		$h_d = 60$	
	TL	DM	TL	DM	TL	DM	TL	DM	TL	DM
Panel A. Before COVID-19 (2007Q1 to 2019Q4)										
$GaR^{ISPREAD}$	2.232	**0.978**	2.072	**0.990**	1.768	**0.988**	1.772	**0.997**	1.692	**0.996**
GaR^{EEFR}	2.000	**0.965**	2.392	**0.935**	1.819	**0.972**	1.711	**0.971**	1.649	**0.968**
GaR^{RET}	2.107	**0.973**	2.049	**0.962**	1.792	**0.946**	2.200	**0.994**	1.594	**0.971**
GaR^{SMB}	2.079	**0.991**	2.202	**0.991**	1.833	**0.994**	1.930	**0.986**	2.069	**0.990**
GaR^{HML}	2.200	**0.957**	1.447	**0.916**	1.570	**0.973**	1.514	**0.968**	1.655	**0.916**
GaR^{MOM}	1.448	**0.987**	2.076	**0.959**	1.578	**0.987**	2.072	**0.960**	1.756	**0.973**
GaR^{VXO}	1.813	**0.991**	1.550	**0.995**	1.521	**0.997**	1.258	**0.921**	1.268	**0.886**
$GaR^{CSPREAD}$	2.242	**0.979**	1.789	**0.993**	1.367	**1.000**	1.275	**0.963**	1.259	**0.951**
GaR^{TERM}	2.198	**0.984**	1.946	**0.991**	1.728	**0.989**	1.754	**0.990**	1.684	**0.989**
GaR^{TED}	1.643	**0.918**	1.603	**0.968**	1.485	**0.964**	1.440	**0.960**	1.397	**0.931**
GaR^{ADS}	1.678	**0.950**	1.496	**0.910**	1.175	**0.717**	0.939	**0.375**	1.263	**0.915**
Panel B. Including COVID-19 (2007Q1 to 2020Q4)										
$GaR^{ISPREAD}$	1.445	**0.968**	1.555	**0.995**	1.530	**0.990**	1.837	**0.973**	1.346	**0.983**
GaR^{EEFR}	1.449	**0.982**	1.707	**0.992**	1.550	**0.987**	1.855	**0.963**	1.367	**0.979**
GaR^{RET}	1.408	**0.992**	1.556	**0.989**	1.503	**0.976**	1.776	**0.964**	1.208	**0.957**
GaR^{SMB}	1.271	**0.948**	1.510	**0.989**	1.301	**0.991**	1.667	**0.960**	1.302	**0.996**
GaR^{HML}	1.453	**0.995**	1.504	**0.983**	1.281	**0.913**	1.834	**0.942**	1.300	**0.975**
GaR^{MOM}	1.274	**0.981**	1.712	**0.971**	1.510	**0.969**	1.722	**0.934**	1.307	**0.988**
GaR^{VXO}	1.196	**0.908**	1.335	**0.995**	1.317	**0.994**	1.426	**0.893**	1.129	**0.950**
$GaR^{CSPREAD}$	1.336	**0.991**	1.351	**0.993**	1.280	**0.939**	1.501	**0.888**	1.133	**0.956**
GaR^{TERM}	1.42	**0.974**	1.502	**0.995**	1.432	**0.993**	1.789	**0.971**	1.334	**0.989**
GaR^{TED}	1.315	**0.960**	1.433	**0.994**	1.420	**0.985**	1.731	**0.950**	1.279	**0.980**
GaR^{ADS}	1.375	**0.923**	0.595	**0.174**	0.655	**0.159**	0.504	**0.152**	0.743	**0.260**

Note: This table shows the TL for each individual GaR forecast relative to the combined GaR forecast, for different daily horizons. We also report the p-values of the DM test for the null hypothesis of equality of forecasts, conducted on a one-sided basis, such that the alternative hypothesis is that the indicated forecast is more accurate than the combined GaR (non-rejection of the null is preferred). If the p-value is above 0.10 (bold values), we conclude that the forecast from the combined GaR is more accurate than that of the individual GaR.

regressions. Furthermore, when comparing our combined GaR framework with that of the standard GaR using a financial condition index (specifically the CISS), we show that our framework performs significantly better. This is also true when comparing our combined GaR framework with different individual GaR specifications, although the performance of those that only include the ADS index is similar when considering the Covid-19 period. This

Table 5: LASSO-Q out-of-sample forecast accuracy based on coverage tests

	$h_d = 0$		$h_d = 10$		$h_d = 20$		$h_d = 40$		$h_d = 60$	
	UC	DQ	UC	DQ	UC	DQ	UC	DQ	UC	DQ
Panel A. Before COVID-19 (2007Q1 to 2019Q4)										
$GaR^{ISPREAD}$	**0.926**	**0.161**	**0.926**	0.072	**0.926**	**0.121**	**0.565**	0.070	**0.565**	**0.052**
GaR^{EEFR}	**0.717**	**0.131**	**0.226**	0.012	**0.427**	0.070	**0.226**	0.089	**0.107**	0.014
GaR^{RET}	**0.226**	0.001	0.001	0.000	0.046	0.000	0.046	0.000	0.001	0.000
GaR^{SMB}	0.046	0.001	**0.427**	0.015	**0.226**	**0.103**	0.006	0.001	**0.107**	0.002
GaR^{HML}	0.046	0.050	**0.107**	0.000	**0.226**	0.001	0.018	0.006	0.018	0.003
GaR^{MOM}	**0.427**	**0.781**	**0.717**	**0.146**	0.046	0.099	0.046	0.000	**0.226**	0.003
GaR^{VXO}	**0.107**	0.066	0.046	**0.812**	0.018	0.063	0.046	0.067	0.046	**0.707**
$GaR^{CSPREAD}$	**0.226**	0.036	**0.226**	0.038	**0.717**	**0.741**	**0.717**	**0.799**	**0.565**	**0.921**
GaR^{TERM}	**0.565**	0.087	**0.565**	0.088	**0.565**	0.080	**0.926**	**0.280**	**0.273**	**0.701**
GaR^{TED}	**0.226**	0.011	**0.107**	0.003	**0.107**	0.003	0.046	0.003	0.046	0.023
GaR^{ADS}	**0.107**	0.067	0.018	0.050	**0.107**	0.043	**0.226**	**0.186**	**0.226**	**0.230**
Panel B. Including COVID-19 (2007Q1 to 2020Q4)										
$GaR^{ISPREAD}$	**0.312**	0.003	**0.312**	0.002	**0.312**	0.002	**0.547**	0.001	**0.547**	0.001
GaR^{EEFR}	**0.160**	0.007	0.031	0.000	0.074	0.001	0.031	0.002	0.012	0.000
GaR^{RET}	0.074	0.000	0.000	0.000	0.004	0.000	0.004	0.000	0.000	0.000
GaR^{SMB}	0.012	0.001	**0.160**	0.004	0.074	0.083	0.001	0.000	0.031	0.001
GaR^{HML}	0.004	0.000	0.012	0.000	0.031	0.001	0.001	0.000	0.004	0.002
GaR^{MOM}	**0.160**	**0.425**	**0.160**	0.018	0.004	0.001	0.004	0.000	0.074	0.000
GaR^{VXO}	0.031	**0.338**	0.004	**0.267**	0.001	0.011	0.004	0.042	0.004	**0.215**
$GaR^{CSPREAD}$	0.031	0.005	0.031	0.011	**0.160**	**0.204**	**0.160**	**0.427**	**0.547**	**0.921**
GaR^{TERM}	**0.547**	0.002	**0.547**	0.001	**0.547**	0.002	**0.312**	0.008	**0.860**	0.021
GaR^{TED}	0.031	0.003	0.012	0.000	0.012	0.000	0.004	0.000	0.004	0.001
GaR^{ADS}	0.074	**0.137**	0.004	0.003	0.031	0.001	0.074	**0.230**	0.031	0.018

Note: This table shows the following two interval tests for different combined GaR models: Kupiec's (1995) unconditional coverage test (UC), where the null hypothesis is that the proportion of exceedances is equal to the quantile (non-rejection of the null is preferred); and the dynamic quantile test (DQ) of Engle and Manganelli (2004), where the null hypothesis is that the exceedance indicator is an i.i.d. process (non-rejection of the null is preferred). Bold values indicate that model passes the test with a 10% level of probability.

evidence suggests that financial variables alone played a limited role in gauging the downside risk for GDP during the Covid-19 pandemic and highlights the complex ways in which real and financial variables interconnect to determine economic growth in what is a causal fashion.

5 Conclusions

We show that both real and financial variables reported with a daily frequency provide valuable information for monitoring periods of economic vulnerability. Here, our main contribution has been to demonstrate that by incorporating both types of variable simultaneously in the GaR framework, it is possible to provide an early warning of a downturn in GDP in pseudo real-time and that this framework works well for both the GFC and the Covid-19 episode.

The flexible approach reported allows us to emphasize the importance of both economic theory and economic intuition when interpreting the results of forecast combinations and for improving the point forecast itself. By acknowledging the complexity of the nowcasting task in macroeconomics, especially when using high-frequency data, we contribute to a better understanding of the economic signals that can be extracted from this daily information when seeking to anticipate downturns in the economy. More specifically, here, we show that during the GFC and the Covid-19 pandemic, the optimal forecasting weights of real and financial variables underwent a marked change. In the earlier of these two periods, financial indicators such as credit spreads and the VXO were fundamental; however, they failed to capture the magnitude of the decline in GDP observed with the onset of the Covid-19 pandemic. This difference in behaviour is attributable to the specific nature of each of the two crises, something we can only grasp because we understand (to some extent) the economic mechanisms underpinning these two events.

Interestingly, among the set of financial variables, VXO and CSPREAD are especially relevant for all models during the GFC, highlighting the prominent role played by uncertainty in determining economic outcomes. However, as discussed, the financial indicators alone were unable to forecast low quantiles of GDP growth during the Covid-19 pandemic. Indeed, only by including the ADS index were we able to gauge both the sign and magnitude of the downside GDP risk in this period.

We show that our combined GaR model outperforms the standard GaR model, which only takes financial indicators into consideration (Adrian et al., 2019; Ferrara et al., 2022). We have been able to evaluate this outcome by comparing the performance of combined GaR nowcasts with that of i) individual GaR nowcasts using the CISS as a benchmark; and ii) individual GaR nowcasts using different financial and real indicators relative to the combined GaR nowcasts. Our specific implementation uses different dimension reduction techniques including MIDAS and shrinkage.

In this study, we have compared seven different models and 12 high-frequency predictors using a forecast combination approach with time-varying optimal weights. In addition, we have used a novel approach based on adaptive sparse group LASSO for quantile regres-

sions, which allows for multiple groups and sparsity within the high-frequency lagged vector (Mendez-Civieta et al., 2021). While this model presents some good properties for addressing high-dimensional problems, we found that LASSO-Q tends to outperform the rest of the models in terms of forecast accuracy at different daily horizons. This is probably a consequence of traditional MIDAS restrictions on the lag structure of the high-frequency indicator, which do not necessarily improve forecast accuracy. As such, our results lend further support to past evidence, inasmuch as shrinkage models should ideally be used to select the number of lags of the highfrequency predictors. Additionally, the ASGL-Q model displays more stable weights than those displayed by the LASSO-Q model, which is arguably a potential cause of the difference in accuracy. Nonetheless, these two weighting schemes emphasize the importance of the ADS indicator for forecasting during the Covid-19 period. Here, we used a single indicator to capture the role of real economic activity - that is, the ADS index - essentially because it is the only that is available at a daily frequency. We also introduced weekly vintages of this indicator to perform the nowcasting exercise in pseudo real-time. Nevertheless, we believe that more indicators gauging the informational content of different facets of economic activity and the credit markets will prove to be fundamental in the future, not only for achieving greater forecasting accuracy in real time, but also for understanding the causes of ongoing crises, before, that is, the actual causal mechanisms become clear to the professionals. In short, our models can be considered as making a contribution to anticipating and understanding economic dangers while the latter are actually unfolding.

References

Adrian, T., Boyarchenko, N., and Giannone, D. (2019). Vulnerable growth. *American Economic Review*, 109(4):1263–1289.

Ahn, S. C. and Horenstein, A. R. (2013). Eigenvalue Ratio Test for the Number of Factors. *Econometrica*, 81(3):1203–1227.

Amburgey, A. J. and McCracken, M. W. (2022). On the real-time predictive content of financial condition indices for growth. *Journal of Applied Econometrics*.

Andreou, E., Ghysels, E., and Kourtellos, A. (2013). Should Macroeconomic Forecasters Use Daily Financial Data and How? *Journal of Business & Economic Statistics*, 31(2):240–251.

Aruoba, S. B., Diebold, F. X., and Scotti, C. (2009). Real-Time Measurement of Business Conditions. *Journal of Business & Economic Statistics*, 27(4):417–427.

Athey, S. (2017). Beyond prediction: Using big data for policy problems. *Science*, 355(6324):483–485.

Bai, J. and Ng, S. (2008). Forecasting economic time series using targeted predictors. *Journal of Econometrics*, 146(2):304–317.

Belloni, A. and Chernozhukov, V. (2011). 1-penalized quantile regression in high-dimensional sparse models. *Annals of Statistics*, 39(1):82–130.

Brownlees, C. and Souza, A. B. (2021). Backtesting global Growth-at-Risk. *Journal of Monetary Economics*, 118:312–330.

Brunnermeier, M. K. and Sannikov, Y. (2016). Macro, Money, and Finance: A Continuous-Time Approach. *Handbook of Macroeconomics*, 2:1497–1545.

Carriero, A., Clark, T. E., and Marcellino, M. (2022). Nowcasting tail risk to economic activity at a weekly frequency. *Journal of Applied Econometrics*, 37(5):843–866.

Christoffersen, P. F. (1998). Evaluating Interval Forecasts. *International Economic Review*, 39(4):841.

Clark, T. and McCracken, M. (2013). Advances in Forecast Evaluation. *Handbook of Economic Forecasting*, 2:1107–1201.

Corradi, V. and Swanson, N. R. (2006). Chapter 5 Predictive Density Evaluation. *Handbook of Economic Forecasting*, 1:197–284.

De Santis, R. A. and Van der Veken, W. (2020). Forecasting macroeconomic risk in real time: Great and Covid-19 Recessions. *ECB Working Paper Series*, (No 2436 / July 2020).

Diebold, F. X. and Mariano, R. S. (1995). Comparing predictive accuracy. *Journal of Business and Economic Statistics*, 13(3):253–263.

Engle, R. F. and Manganelli, S. (2004). CAViaR. *Journal of Business & Economic Statistics*, 22(4):367–381.

Estrella, A. and Mishkin, F. S. (1998). Predicting U.S. Recessions: Financial Variables as Leading Indicators. *The Review of Economics and Statistics*, 80(1):45–61.

Fama, E. F. and French, K. R. (1993). Common risk factors in the returns on stocks and bonds. *Journal of Financial Economics*, 33(1):3–56.

Faust, J., Gilchrist, S., Wright, J. H., and Zakrajšek, E. (2013). Credit Spreads as Predictors of Real-Time Economic Activity: A Bayesian Model-Averaging Approach. *The Review of Economics and Statistics*, 95(5):1501–1519.

Ferrara, L., Mogliani, M., and Sahuc, J. G. (2022). High-frequency monitoring of growth at risk. *International Journal of Forecasting*, 38(2):582–595.

Figueres, J. M. and Jarociński, M. (2020). Vulnerable growth in the euro area: Measuring the financial conditions. *Economics Letters*, 191:109126.

Friedman, J., Hastie, T., and Tibshirani, R. (2010). Regularization Paths for Generalized Linear Models via Coordinate Descent. *Journal of Statistical Software*, 33(1):1–22.

Gertler, M. and Gilchrist, S. (2018). What Happened: Financial Factors in the Great Recession. *Journal of Economic Perspectives*, 32(3):3–30.

Ghysels, E., Plazzi, A., and Valkanov, R. (2016). Why Invest in Emerging Markets? The Role of Conditional Return Asymmetry. *Journal of Finance*, 71(5):2145–2192.

Giacomini, R. and Komunjer, I. (2005). Evaluation and Combination of Conditional Quantile Forecasts. *Journal of Business & Economic Statistics*, 23(4):416–431.

Giglio, S., Kelly, B., and Pruitt, S. (2016). Systemic risk and the macroeconomy: An empirical evaluation. *Journal of Financial Economics*, 119(3):457–471.

Gneiting, T. and Raftery, A. E. (2007). Strictly Proper Scoring Rules, Prediction, and Estimation. *Journal of the American Statistical Association*, 102(477):359–378.

Gneiting, T. and Ranjan, R. (2011). Comparing Density Forecasts Using Threshold- and Quantile-Weighted Scoring Rules. *Journal of Business & Economic Statistics*, 29(3):411–422.

Guerrieri, V., Lorenzoni, G., Straub, L., and Werning, I. (2022). Macroeconomic Implications of COVID-19: Can Negative Supply Shocks Cause Demand Shortages? *American Economic Review*, 112(5):1437–74.

Gunay, S. (2020). Seeking causality between liquidity risk and credit risk: TED-OIS spreads and CDS indexes. *Research in International Business and Finance*, 52:101189.

Hansen, P. R., Lunde, A., and Nason, J. M. (2011). The Model Confidence Set. *Econometrica*, 79(2):453–497.

Harvey, D., Leybourne, S., and Newbold, P. (1997). Testing the equality of prediction mean squared errors. *International Journal of Forecasting*, 13(2):281–291.

Holló, D., Kremer, M., and Lo Duca, M. (2012). CISS - A Composite Indicator of Systemic Stress in the Financial System. *Working Paper Series*, 1426.

Isohätälä, J., Klimenko, N., and Milne, A. (2016). Post-Crisis Macrofinancial Modeling: Continuous Time Approaches. *The Handbook of Post Crisis Financial Modeling*, pages 235–282.

Koenker, R. (2005). *Quantile regression*. Cambridge University Press.

Koenker, R. and Bassett, G. (1978). Regression Quantiles. *Econometrica*, 46(1):33.

Kozumi, H. and Kobayashi, G. (2011). Gibbs sampling methods for Bayesian quantile regression. *Journal of Statistical Computation and Simulation*, 81(11):1565–1578.

Kupiec, P. H. (1995). Techniques for Verifying the Accuracy of Risk Measurement Models. *The Journal of Derivatives*, 3(2):73–84.

Lima, L. R. and Meng, F. (2017). Out-of-Sample Return Predictability: A Quantile Combination Approach. *Journal of Applied Econometrics*, 32(4):877–895.

Lima, L. R., Meng, F., and Godeiro, L. (2020). Quantile forecasting with mixed-frequency data. *International Journal of Forecasting*, 36(3):1149–1162.

Longstaff, F. A., Pan, J., Pedersen, L. H., and Singleton, K. J. (2011). How Sovereign Is Sovereign Credit Risk? *American Economic Journal: Macroeconomics*, 3(2):75–103.

Maldonado, J. and Ruiz, E. (2021). Accurate Confidence Regions for Principal Components Factors*. *Oxford Bulletin of Economics and Statistics*, 83(6):1432–1453.

Manzan, S. (2015). Forecasting the Distribution of Economic Variables in a Data-Rich Environment. *Journal of Business & Economic Statistics*, 33(1):144–164.

Mendez-Civieta, A., Aguilera-Morillo, M. C., and Lillo, R. E. (2021). Adaptive sparse group LASSO in quantile regression. *Advances in Data Analysis and Classification*, 15(3).

Mogliani, M. and Simoni, A. (2021). Bayesian MIDAS penalized regressions: Estimation, selection, and prediction. *Journal of Econometrics*, 222(1):833–860.

Pettenuzzo, D., Timmermann, A., and Valkanov, R. (2016). A MIDAS approach to modeling first and second moment dynamics. *Journal of Econometrics*, 193(2):315–334.

Plagborg-Møller, M., Reichlin, L., Ricco, G., and Hasenzagl, T. (2020). When Is Growth at Risk? *Brookings Papers on Economic Activity*, 2020(1):167–229.

Prasad, A., Elekdag, S., Jeasakul, P., Lafarguette, R., Alter, A., Xiaochen Feng, A., and Wang, C. (2019). Growth at Risk: Concept and Application in IMF Country Surveillance. *IMF Working Papers*, 19(36):1.

Reichlin, L., Ricco, G., and Hasenzagl, T. (2020). Financial Variables as Predictors of Real Growth Vulnerability. *Documents de Travail de l'OFCE*.

Rey, H. (2015). Dilemma not Trilemma: The Global Financial Cycle and Monetary Policy Independence. *CEPR Discussion Papers*.

Stock, J. H. and Watson, M. W. (2004). Combination forecasts of output growth in a seven-country data set. *Journal of Forecasting*, 23(6):405–430.

Yang, Y., Wang, H. J., and He, X. (2015). Posterior Inference in Bayesian Quantile Regression with Asymmetric Laplace Likelihood. *International Statistical Review*, 84(3):327–344.

Yu, K. and Moyeed, R. A. (2001). Bayesian quantile regression. *Statistics & Probability Letters*, 54(4):437–447.

Zou, H. (2006). The adaptive lasso and its oracle properties. *Journal of the American Statistical Association*, 101(476).

Zou, H. and Hastie, T. (2005). Regularization and variable selection via the elastic net. *Journal of the Royal Statistical Society: Series B (Statistical Methodology)*, 67(2):301–320.

A Appendix A

Figure 1A.1: Selected high-frequency LASSO-Q lags from individual GaR specifications

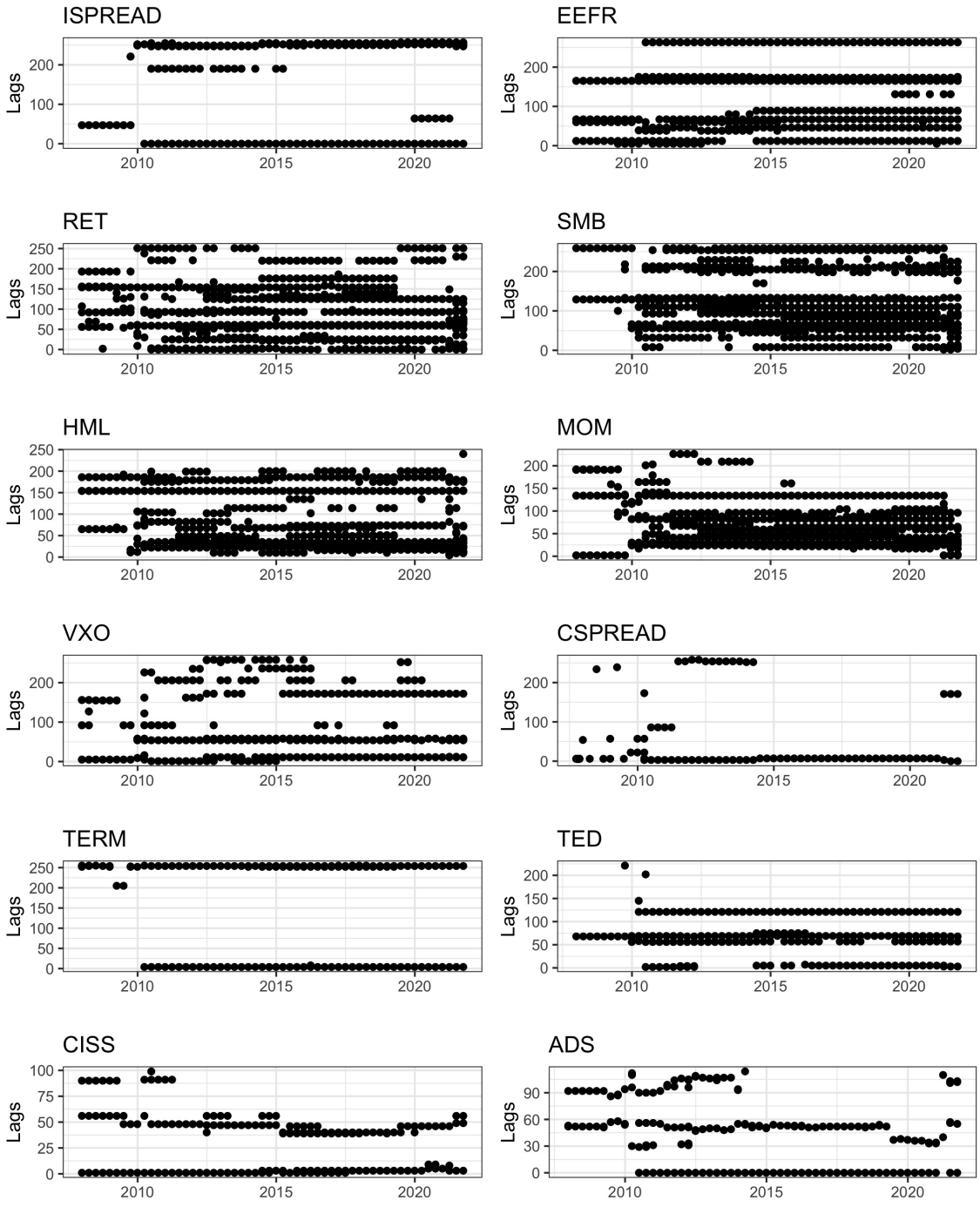

Note: The figure shows selected daily lags from the individual LASSO-Q models corresponding to the last day of each quarter.

Figure 1A.2: Selected high-frequency EN-Q lags from individual GaR specifications

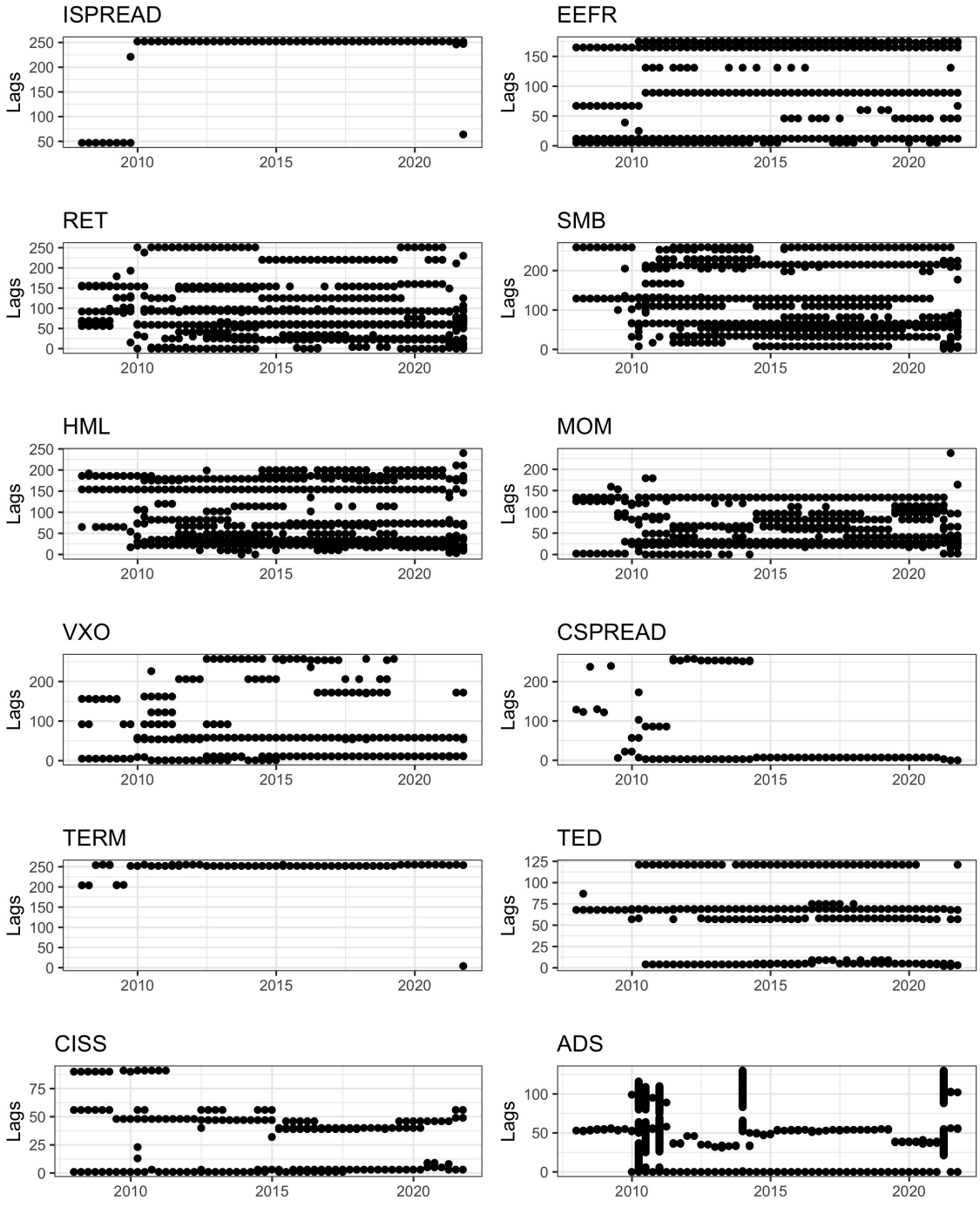

Note: The figure shows selected daily lags from the individual EN-Q models corresponding to the last day of each quarter.

Figure 1A.3: Daily forecast combination weights

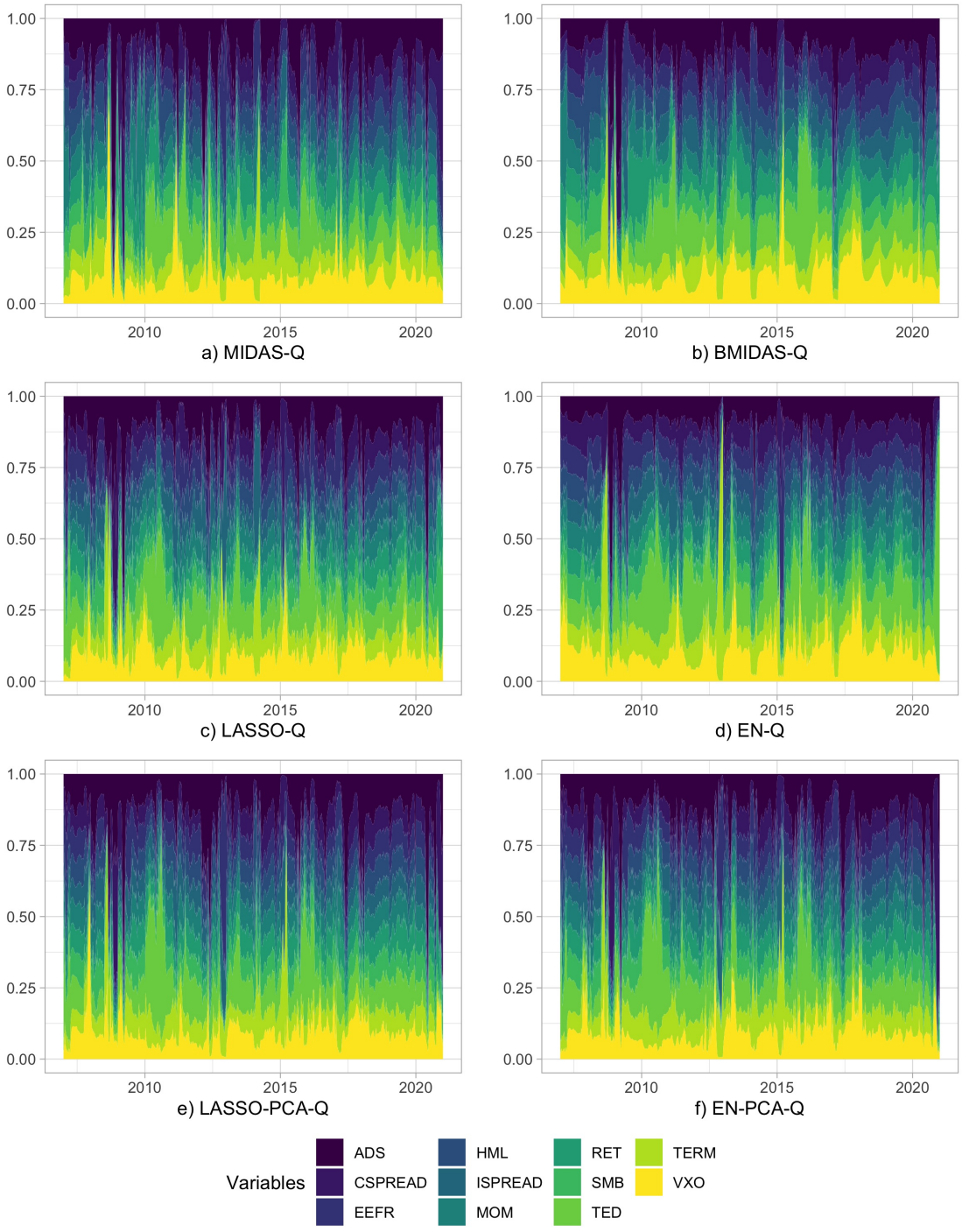

Note: The estimation sample spans the period from 1986Q1 to 2020Q4, and the daily nowcasts commence as of 1 January 2007.

B Appendix B

Table 2B.1: MIDAS-Q out-of-sample forecast accuracy based on the relative TL

	$h_d = 0$		$h_d = 10$		$h_d = 20$		$h_d = 40$		$h_d = 60$	
	TL	DM	TL	DM	TL	DM	TL	DM	TL	DM
Panel A. Before COVID-19 (2007Q1 to 2019Q4)										
$GaR^{ISPREAD}$	2.338	**0.990**	2.285	**0.990**	2.313	**0.99**	2.212	**0.991**	2.234	**0.987**
GaR^{EEFR}	2.317	**0.971**	2.185	**0.962**	2.221	**0.967**	2.12	**0.968**	1.999	**0.955**
GaR^{RET}	1.446	**0.989**	1.506	**0.994**	1.595	**0.997**	1.808	**0.996**	1.637	**0.996**
GaR^{SMB}	2.11	**0.988**	2.124	**0.991**	2.07	**0.993**	2.008	**0.992**	2.058	**0.989**
GaR^{HML}	2.141	**0.987**	2.204	**0.986**	2.29	**0.978**	2.452	**0.980**	2.169	**0.981**
GaR^{MOM}	2.097	**0.978**	1.987	**0.978**	1.945	**0.979**	1.752	**0.978**	1.780	**0.974**
GaR^{VXO}	1.617	**0.951**	1.589	**0.959**	1.537	**0.975**	1.493	**0.986**	1.467	**0.994**
$GaR^{CSPREAD}$	2.052	**0.996**	1.834	**0.997**	1.579	**1.000**	1.363	**0.997**	1.414	**1.000**
GaR^{TERM}	2.313	**0.989**	2.253	**0.989**	2.252	**0.988**	2.173	**0.991**	2.198	**0.987**
GaR^{TED}	1.957	**0.982**	1.929	**0.978**	1.889	**0.977**	1.758	**0.980**	1.784	**0.981**
GaR^{ADS}	1.474	**0.936**	1.527	**0.953**	1.377	**0.928**	1.100	**0.698**	1.433	**0.908**
Panel B. Including COVID-19 (2007Q1 to 2020Q4)										
$GaR^{ISPREAD}$	1.437	**0.996**	1.470	**0.998**	1.489	**0.992**	2.201	**0.952**	1.334	**0.991**
GaR^{EEFR}	1.327	**0.988**	1.375	**0.984**	1.418	**0.969**	2.087	**0.923**	1.231	**0.969**
GaR^{RET}	1.370	**0.977**	1.460	**0.984**	1.494	**0.981**	2.235	**0.951**	1.327	**0.954**
GaR^{SMB}	1.491	**0.990**	1.539	**0.993**	1.537	**0.985**	2.267	**0.951**	1.355	**0.985**
GaR^{HML}	1.585	**0.989**	1.650	**0.996**	1.633	**0.997**	2.433	**0.966**	1.433	**0.996**
GaR^{MOM}	1.664	**0.970**	1.698	**0.975**	1.729	**0.972**	2.453	**0.959**	1.511	**0.948**
GaR^{VXO}	1.202	**0.935**	1.251	**0.961**	1.300	**0.960**	1.918	**0.927**	1.107	**0.892**
$GaR^{CSPREAD}$	1.300	**0.995**	1.307	**0.991**	1.270	**0.946**	1.819	**0.871**	1.115	**0.984**
GaR^{TERM}	1.438	**0.995**	1.471	**0.997**	1.486	**0.990**	2.18	**0.948**	1.318	**0.990**
GaR^{TED}	1.407	**0.994**	1.454	**0.993**	1.465	**0.984**	2.113	**0.935**	1.276	**0.987**
GaR^{ADS}	1.089	**0.796**	0.788	**0.247**	0.762	**0.248**	0.764	**0.231**	0.978	**0.446**

Note: This table shows the TL for each combined GaR relative to the individual GaR considering the CISS, for different daily horizons. We also report the p-values of the DM test for the null hypothesis of equality of forecasts, conducted on a one-sided basis, such that the alternative hypothesis is that the indicated forecast is more accurate than the benchmark (a rejection of the null is preferred). If the p-value is below 0.10 (bold values), we conclude that the forecast from a combined GaR model is more accurate than that of the benchmark.

Table 2B.2: BMIDAS-Q out-of-sample forecast accuracy based on the relative TL

	$h_d = 0$		$h_d = 10$		$h_d = 20$		$h_d = 40$		$h_d = 60$	
	TL	DM	TL	DM	TL	DM	TL	DM	TL	DM
Panel A. Before COVID-19 (2007Q1 to 2019Q4)										
$GaR^{ISPREAD}$	2.133	**0.972**	2.109	**0.971**	2.075	**0.970**	2.054	**0.970**	2.026	**0.967**
GaR^{EEFR}	1.892	**0.969**	1.842	**0.965**	1.802	**0.964**	1.799	**0.965**	1.685	**0.956**
GaR^{RET}	1.259	**0.966**	1.348	**0.989**	1.331	**0.975**	1.333	**0.969**	1.346	**0.973**
GaR^{SMB}	2.217	**0.978**	2.215	**0.979**	2.160	**0.981**	2.181	**0.977**	2.152	**0.977**
GaR^{HML}	2.15	**0.965**	2.227	**0.965**	2.265	**0.954**	2.432	**0.948**	2.058	**0.942**
GaR^{MOM}	2.706	**0.979**	2.546	**0.983**	2.325	**0.984**	2.101	**0.972**	2.100	**0.980**
GaR^{VXO}	1.378	**0.959**	1.360	**0.965**	1.335	**0.970**	1.311	**0.971**	1.245	**0.957**
$GaR^{CSPREAD}$	1.561	**1.000**	1.544	**1.000**	1.528	**1.000**	1.519	**1.000**	1.493	**1.000**
GaR^{TERM}	2.163	**0.973**	2.128	**0.971**	2.089	**0.970**	2.068	**0.970**	2.056	**0.969**
GaR^{TED}	1.488	**0.917**	1.458	**0.916**	1.421	**0.914**	1.395	**0.930**	1.374	**0.935**
GaR^{ADS}	1.177	**0.908**	1.197	**0.935**	1.125	**0.884**	0.961	**0.330**	1.119	**0.784**
Panel B. Including COVID-19 (2007Q1 to 2020Q4)										
$GaR^{ISPREAD}$	1.342	**0.989**	1.368	**0.991**	1.367	**0.977**	2.054	**0.923**	1.245	**0.972**
GaR^{EEFR}	1.232	**0.982**	1.248	**0.983**	1.26	**0.960**	1.909	**0.910**	1.135	**0.934**
GaR^{RET}	1.183	**0.951**	1.26	**0.969**	1.248	**0.947**	1.834	**0.877**	1.117	**0.980**
GaR^{SMB}	1.392	**0.993**	1.414	**0.991**	1.403	**0.975**	2.150	**0.928**	1.295	**0.983**
GaR^{HML}	1.435	**0.983**	1.491	**0.990**	1.496	**0.985**	2.268	**0.945**	1.304	**0.975**
GaR^{MOM}	1.51	**0.991**	1.488	**0.995**	1.445	**0.994**	2.094	**0.933**	1.285	**0.990**
GaR^{VXO}	1.039	**0.720**	1.067	**0.894**	1.112	**0.927**	1.704	**0.892**	1.009	**0.545**
$GaR^{CSPREAD}$	1.194	**0.991**	1.227	**0.998**	1.229	**0.985**	1.850	**0.902**	1.127	**1.000**
GaR^{TERM}	1.354	**0.990**	1.377	**0.991**	1.376	**0.977**	2.073	**0.925**	1.26	**0.977**
GaR^{TED}	1.242	**0.969**	1.263	**0.969**	1.257	**0.935**	1.885	**0.882**	1.142	**0.964**
GaR^{ADS}	1.000	**0.501**	0.754	**0.204**	0.742	**0.215**	0.689	**0.196**	0.907	**0.305**

Note: This table shows the TL for each combined GaR relative to the individual GaR considering the CISS, for different daily horizons. We also report the p-values of the DM test for the null hypothesis of equality of forecasts, conducted on a one-sided basis, such that the alternative hypothesis is that the indicated forecast is more accurate than the benchmark (a rejection of the null is preferred). If the p-value is below 0.10 (bold values), we conclude that the forecast from a combined GaR model is more accurate than that of the benchmark.

Table 2B.3: EN-Q out-of-sample forecast accuracy based on the relative TL

	$h_d = 0$		$h_d = 10$		$h_d = 20$		$h_d = 40$		$h_d = 60$	
	TL	DM	TL	DM	TL	DM	TL	DM	TL	DM
Panel A. Before COVID-19 (2007Q1 to 2019Q4)										
$GaR^{ISPREAD}$	1.339	**0.988**	1.327	**0.992**	1.305	**0.991**	1.462	**0.981**	1.456	**0.976**
GaR^{EEFR}	1.373	**0.959**	1.569	**0.919**	1.41	**0.956**	1.564	**0.969**	1.549	**0.959**
GaR^{RET}	1.589	**0.992**	1.536	**0.971**	1.919	**0.992**	1.732	**0.98**	2.263	**0.986**
GaR^{SMB}	1.308	**1.000**	1.362	**1.000**	1.611	**0.992**	1.756	**0.997**	1.681	**0.996**
GaR^{HML}	1.631	**0.991**	1.182	**0.925**	1.289	**0.993**	1.854	**0.997**	1.809	**0.993**
GaR^{MOM}	1.050	**0.808**	1.355	**0.950**	1.312	**0.989**	1.870	**0.984**	1.450	**0.951**
GaR^{VXO}	1.315	**0.974**	1.328	**0.979**	1.293	**0.970**	1.257	**0.890**	1.284	**0.924**
$GaR^{CSPREAD}$	1.170	**0.907**	1.177	**0.934**	1.144	**0.911**	1.303	**0.961**	1.250	**0.955**
GaR^{TERM}	1.273	**0.987**	1.255	**0.993**	1.253	**0.994**	1.427	**0.974**	1.398	**0.971**
GaR^{TED}	1.200	**0.830**	1.195	**0.853**	1.181	**0.855**	1.364	**0.915**	1.261	**0.845**
GaR^{ADS}	1.038	**0.589**	1.038	**0.588**	0.96	**0.405**	0.865	**0.230**	1.048	**0.672**
Panel B. Including COVID-19 (2007Q1 to 2020Q4)										
$GaR^{ISPREAD}$	1.165	**0.967**	1.151	**0.988**	1.33	**0.955**	1.926	**0.906**	1.202	**0.993**
GaR^{EEFR}	1.216	**0.981**	1.261	**0.977**	1.382	**0.953**	1.983	**0.910**	1.159	**0.976**
GaR^{RET}	1.414	**0.988**	1.381	**0.988**	1.649	**0.972**	1.992	**0.911**	1.414	**0.991**
GaR^{SMB}	1.203	**0.980**	1.429	**0.989**	1.409	**0.986**	2.108	**0.921**	1.268	**0.992**
GaR^{HML}	1.367	**0.994**	1.436	**0.980**	1.179	**0.975**	2.634	**0.951**	1.266	**0.996**
GaR^{MOM}	1.222	**0.952**	1.374	**0.982**	1.439	**0.949**	2.247	**0.931**	1.196	**0.973**
GaR^{VXO}	1.078	**0.926**	1.127	**0.992**	1.264	**0.931**	1.839	**0.877**	1.135	**0.959**
$GaR^{CSPREAD}$	1.152	**0.952**	1.132	**0.972**	1.293	**0.877**	1.845	**0.872**	1.114	**0.928**
GaR^{TERM}	1.145	**0.945**	1.157	**0.985**	1.35	**0.958**	1.988	**0.918**	1.187	**0.989**
GaR^{TED}	1.140	**0.911**	1.155	**0.960**	1.316	**0.903**	1.927	**0.885**	1.132	**0.923**
GaR^{ADS}	0.961	**0.380**	0.809	**0.169**	0.672	**0.146**	0.733	**0.190**	0.845	**0.316**

Note: This table shows the TL for each combined GaR relative to the individual GaR considering the CISS, for different daily horizons. We also report the p-values of the DM test for the null hypothesis of equality of forecasts, conducted on a one-sided basis, such that the alternative hypothesis is that the indicated forecast is more accurate than the benchmark (a rejection of the null is preferred). If the p-value is below 0.10 (bold values), we conclude that the forecast from a combined GaR model is more accurate than that of the benchmark.

Table 2B.4: LASSO-PCA-Q out-of-sample forecast accuracy based on the relative TL

	$h_d = 0$		$h_d = 10$		$h_d = 20$		$h_d = 40$		$h_d = 60$	
	TL	DM	TL	DM	TL	DM	TL	DM	TL	DM
Panel A. Before COVID-19 (2007Q1 to 2019Q4)										
$GaR^{ISPREAD}$	2.200	**0.978**	2.260	**0.988**	1.868	**0.988**	1.723	**0.997**	1.678	**0.996**
GaR^{EEFR}	2.254	**0.961**	2.295	**0.957**	2.074	**0.973**	1.795	**0.974**	1.822	**0.976**
GaR^{RET}	2.222	**0.980**	2.270	**0.968**	1.777	**0.927**	2.197	**0.984**	1.544	**0.978**
GaR^{SMB}	2.288	**0.992**	1.851	**0.971**	1.826	**0.988**	1.649	**0.981**	1.588	**0.989**
GaR^{HML}	2.163	**0.940**	2.425	**0.957**	1.938	**0.960**	2.188	**0.988**	1.726	**0.942**
GaR^{MOM}	1.475	**0.995**	1.958	**0.95**	1.622	**0.988**	1.976	**0.971**	1.700	**0.989**
GaR^{VXO}	1.785	**0.990**	1.714	**0.994**	1.591	**0.999**	1.328	**0.940**	1.220	**0.867**
$GaR^{CSPREAD}$	2.271	**0.982**	1.939	**0.996**	1.406	**1.000**	1.241	**0.915**	1.227	**0.931**
GaR^{TERM}	2.204	**0.986**	2.105	**0.987**	1.816	**0.987**	1.730	**0.992**	1.656	**0.990**
GaR^{TED}	1.644	**0.923**	1.736	**0.965**	1.562	**0.965**	1.407	**0.951**	1.379	**0.933**
GaR^{ADS}	1.187	**0.847**	1.186	**0.834**	0.928	**0.307**	0.943	**0.374**	1.228	**0.884**
Panel B. Including COVID-19 (2007Q1 to 2020Q4)										
$GaR^{ISPREAD}$	1.418	**0.964**	1.807	**0.994**	2.591	**0.952**	2.139	**0.957**	1.319	**0.977**
GaR^{EEFR}	1.502	**0.969**	1.938	**0.988**	2.834	**0.958**	2.284	**0.955**	1.445	**0.975**
GaR^{RET}	1.392	**0.992**	1.743	**0.974**	2.423	**0.909**	2.070	**0.947**	1.171	**0.981**
GaR^{SMB}	1.239	**0.908**	1.602	**0.952**	2.201	**0.926**	1.857	**0.893**	1.227	**0.995**
GaR^{HML}	1.314	**0.971**	2.051	**0.99**	2.658	**0.964**	3.143	**0.963**	1.209	**0.968**
GaR^{MOM}	1.14	**0.882**	1.990	**0.983**	2.444	**0.912**	2.059	**0.926**	1.208	**0.992**
GaR^{VXO}	1.087	**0.700**	1.480	**0.983**	2.122	**0.921**	1.688	**0.881**	1.090	**0.963**
$GaR^{CSPREAD}$	1.271	**0.963**	1.532	**0.983**	2.139	**0.888**	1.725	**0.874**	1.079	**0.981**
GaR^{TERM}	1.377	**0.956**	1.742	**0.995**	2.385	**0.940**	2.091	**0.952**	1.300	**0.984**
GaR^{TED}	1.274	**0.932**	1.662	**0.988**	2.450	**0.934**	2.018	**0.930**	1.247	**0.978**
GaR^{ADS}	1.499	**0.851**	0.606	**0.139**	0.610	**0.113**	0.605	**0.122**	0.902	**0.301**

Note: This table shows the TL for each combined GaR relative to the individual GaR considering the CISS, for different daily horizons. We also report the p-values of the DM test for the null hypothesis of equality of forecasts, conducted on a one-sided basis, such that the alternative hypothesis is that the indicated forecast is more accurate than the benchmark (a rejection of the null is preferred). If the p-value is below 0.10 (bold values), we conclude that the forecast from a combined GaR model is more accurate than that of the benchmark.

Table 2B.5: EN-PCA-Q out-of-sample forecast accuracy based on the relative TL

	$h_d = 0$		$h_d = 10$		$h_d = 20$		$h_d = 40$		$h_d = 60$	
	TL	DM	TL	DM	TL	DM	TL	DM	TL	DM
Panel A. Before COVID-19 (2007Q1 to 2019Q4)										
$GaR^{ISPREAD}$	2.232	**0.978**	2.072	**0.990**	1.768	**0.988**	1.772	**0.997**	1.692	**0.996**
GaR^{EEFR}	2.000	**0.965**	2.392	**0.935**	1.819	**0.972**	1.711	**0.971**	1.649	**0.968**
GaR^{RET}	2.107	**0.973**	2.049	**0.962**	1.792	**0.946**	2.200	**0.994**	1.594	**0.971**
GaR^{SMB}	2.079	**0.991**	2.202	**0.991**	1.833	**0.994**	1.930	**0.986**	2.069	**0.990**
GaR^{HML}	2.200	**0.957**	1.447	**0.916**	1.57	**0.973**	1.514	**0.968**	1.655	**0.916**
GaR^{MOM}	1.448	**0.987**	2.076	**0.959**	1.578	**0.987**	2.072	**0.960**	1.756	**0.973**
GaR^{VXO}	1.813	**0.991**	1.550	**0.995**	1.521	**0.997**	1.258	**0.921**	1.268	**0.886**
$GaR^{CSPREAD}$	2.242	**0.979**	1.789	**0.993**	1.367	**1.000**	1.275	**0.963**	1.259	**0.951**
GaR^{TERM}	2.198	**0.984**	1.946	**0.991**	1.728	**0.989**	1.754	**0.990**	1.684	**0.989**
GaR^{TED}	1.643	**0.918**	1.603	**0.968**	1.485	**0.964**	1.440	**0.960**	1.397	**0.931**
GaR^{ADS}	1.678	**0.950**	1.496	**0.910**	1.175	**0.717**	0.939	**0.375**	1.263	**0.915**
Panel B. Including COVID-19 (2007Q1 to 2020Q4)										
$GaR^{ISPREAD}$	1.445	**0.968**	1.555	**0.995**	1.530	**0.99**	1.837	**0.973**	1.346	**0.983**
GaR^{EEFR}	1.449	**0.982**	1.707	**0.992**	1.550	**0.987**	1.855	**0.963**	1.367	**0.979**
GaR^{RET}	1.408	**0.992**	1.556	**0.989**	1.503	**0.976**	1.776	**0.964**	1.208	**0.957**
GaR^{SMB}	1.271	**0.948**	1.510	**0.989**	1.301	**0.991**	1.667	**0.960**	1.302	**0.996**
GaR^{HML}	1.453	**0.995**	1.504	**0.983**	1.281	**0.913**	1.834	**0.942**	1.300	**0.975**
GaR^{MOM}	1.274	**0.981**	1.712	**0.971**	1.510	**0.969**	1.722	**0.934**	1.307	**0.988**
GaR^{VXO}	1.196	**0.908**	1.335	**0.995**	1.317	**0.994**	1.426	**0.893**	1.129	**0.950**
$GaR^{CSPREAD}$	1.336	**0.991**	1.351	**0.993**	1.280	**0.939**	1.501	**0.888**	1.133	**0.956**
GaR^{TERM}	1.420	**0.974**	1.502	**0.995**	1.432	**0.993**	1.789	**0.971**	1.334	**0.989**
GaR^{TED}	1.315	**0.960**	1.433	**0.994**	1.420	**0.985**	1.731	**0.950**	1.279	**0.980**
GaR^{ADS}	1.375	**0.923**	0.595	**0.174**	0.655	**0.159**	0.504	**0.152**	0.743	**0.260**

Note: This table shows the TL for each combined GaR relative to the individual GaR considering the CISS, for different daily horizons. We also report the p-values of the DM test for the null hypothesis of equality of forecasts, conducted on a one-sided basis, such that the alternative hypothesis is that the indicated forecast is more accurate than the benchmark (a rejection of the null is preferred). If the p-value is below 0.10 (bold values), we conclude that the forecast from a combined GaR model is more accurate than that of the benchmark.

C Appendix C

Table 3C.1: MIDAS-Q out-of-sample forecast accuracy based on coverage tests

	$h_d = 0$		$h_d = 10$		$h_d = 20$		$h_d = 40$		$h_d = 60$	
	UC	DQ	UC	DQ	UC	DQ	UC	DQ	UC	DQ
Panel A. Before COVID-19 (2007Q1 to 2019Q4)										
$GaR^{ISPREAD}$	**0.565**	0.039	**0.565**	0.042	**0.565**	0.032	**0.565**	0.034	**0.565**	0.032
GaR^{EEFR}	**0.273**	0.003	0.095	**0.142**	**0.273**	0.002	**0.273**	0.003	**0.273**	0.004
GaR^{RET}	**0.427**	**0.452**	**0.226**	**0.713**	0.046	**0.281**	0.046	0.027	0.046	0.015
GaR^{SMB}	**0.926**	**0.200**	**0.717**	**0.509**	**0.717**	**0.553**	**0.926**	**0.191**	**0.926**	0.153
GaR^{HML}	**0.565**	**0.560**	**0.565**	**0.561**	**0.717**	**0.506**	**0.717**	0.077	**0.926**	**0.273**
GaR^{MOM}	**0.926**	**0.142**	**0.926**	0.054	**0.565**	**0.147**	**0.273**	**0.368**	0.095	**0.141**
GaR^{VXO}	**0.926**	**0.903**	**0.717**	**0.878**	**0.717**	**0.867**	**0.717**	**0.863**	**0.226**	**0.887**
$GaR^{CSPREAD}$	**0.717**	0.088	**0.926**	0.090	**0.926**	**0.102**	**0.273**	**0.925**	0.095	**0.826**
GaR^{TERM}	**0.565**	0.056	**0.565**	0.060	**0.273**	0.002	**0.273**	0.002	**0.273**	0.002
GaR^{TED}	**0.226**	**0.273**	**0.107**	**0.265**	**0.226**	**0.309**	**0.226**	**0.310**	**0.226**	**0.323**
GaR^{ADS}	**0.226**	**0.229**	**0.226**	**0.201**	**0.226**	**0.230**	0.006	0.000	**0.107**	0.072
Panel B. Including COVID-19 (2007Q1 to 2020Q4)										
$GaR^{ISPREAD}$	**0.547**	0.001	**0.547**	0.001	**0.547**	0.000	**0.547**	0.000	**0.547**	0.000
GaR^{EEFR}	**0.860**	0.001	**0.786**	0.004	**0.860**	0.000	**0.860**	0.000	**0.860**	0.000
GaR^{RET}	0.074	0.059	0.031	0.015	0.004	0.005	0.004	0.001	0.004	0.001
GaR^{SMB}	**0.312**	0.004	**0.160**	0.014	**0.160**	0.015	**0.312**	0.003	**0.312**	0.003
GaR^{HML}	**0.547**	0.008	**0.547**	0.007	**0.160**	0.007	**0.160**	0.001	**0.312**	0.005
GaR^{MOM}	**0.312**	0.005	**0.312**	0.000	**0.547**	0.004	**0.860**	0.008	**0.786**	0.000
GaR^{VXO}	**0.547**	**0.675**	**0.160**	**0.763**	**0.160**	**0.685**	**0.160**	**0.656**	0.031	**0.584**
$GaR^{CSPREAD}$	**0.160**	0.100	**0.312**	0.035	**0.312**	0.056	**0.860**	**0.626**	**0.786**	**0.405**
GaR^{TERM}	**0.547**	0.001	**0.547**	0.001	**0.860**	0.000	**0.860**	0.000	**0.860**	0.000
GaR^{TED}	0.031	**0.242**	0.012	0.028	0.031	0.033	0.031	0.041	0.031	0.032
GaR^{ADS}	**0.160**	**0.146**	**0.160**	0.088	0.074	0.015	0.004	0.002	0.031	0.008

Note: This table shows the following two interval tests for different combined GaR models: Kupiec's (1995) unconditional coverage test (UC), where the null hypothesis is that the proportion of exceedances is equal to the quantile (non-rejection of the null is preferred); and the dynamic quantile test (DQ) of Engle and Manganelli (2004), where the null hypothesis is that the exceedance indicator is an i.i.d. process (non-rejection of the null is preferred). Bold values indicate that model passes the test with a 10% level of probability.

Table 3C.2: BMIDAS-Q out-of-sample forecast accuracy based on coverage tests

	$h_d = 0$		$h_d = 10$		$h_d = 20$		$h_d = 40$		$h_d = 60$	
	UC	DQ	UC	DQ	UC	DQ	UC	DQ	UC	DQ
Panel A. Before COVID-19 (2007Q1 to 2019Q4)										
$GaR^{ISPREAD}$	0.095	**0.139**	0.095	**0.141**	0.095	**0.142**	0.095	**0.141**	**0.273**	0.012
GaR^{EEFR}	**0.273**	0.006	**0.273**	0.006	0.095	0.082	0.095	**0.109**	0.095	0.074
GaR^{RET}	**0.427**	0.058	**0.926**	**0.682**	**0.565**	**0.877**	**0.427**	**0.638**	**0.717**	**0.383**
GaR^{SMB}	**0.565**	0.000	**0.565**	0.000	**0.565**	0.000	**0.565**	0.000	**0.565**	0.000
GaR^{HML}	**0.565**	0.029	**0.565**	0.022	**0.273**	**0.228**	**0.273**	0.005	**0.273**	**0.139**
GaR^{MOM}	**0.273**	0.012	**0.273**	0.013	**0.273**	0.013	**0.273**	0.012	0.095	**0.125**
GaR^{VXO}	**0.565**	**0.907**	**0.565**	**0.908**	**0.565**	**0.909**	**0.926**	**0.907**	**0.717**	**0.710**
$GaR^{CSPREAD}$	0.095	**0.885**	0.095	**0.881**	0.095	**0.880**	0.095	**0.874**	0.019	0.811
GaR^{TERM}	0.095	**0.139**	0.095	**0.142**	0.095	**0.142**	0.095	**0.14**	**0.273**	0.012
GaR^{TED}	**0.717**	**0.731**	**0.717**	**0.713**	**0.717**	**0.695**	**0.717**	**0.686**	**0.717**	**0.696**
GaR^{ADS}	**0.565**	**0.892**	**0.926**	**0.901**	**0.565**	**0.758**	**0.095**	**0.432**	0.095	**0.375**
Panel B. Including COVID-19 (2007Q1 to 2020Q4)										
$GaR^{ISPREAD}$	**0.455**	0.015	**0.455**	0.015	**0.455**	0.015	**0.455**	0.014	**0.786**	0.004
GaR^{EEFR}	**0.786**	0.000	**0.786**	0.000	**0.455**	0.001	**0.455**	0.004	**0.455**	0.002
GaR^{RET}	**0.160**	**0.140**	**0.547**	**0.163**	**0.860**	**0.362**	**0.16**	**0.168**	**0.312**	0.052
GaR^{SMB}	**0.860**	0.000	**0.860**	0.000	**0.860**	0.000	**0.86**	0.000	**0.860**	0.000
GaR^{HML}	**0.860**	0.001	**0.860**	0.000	**0.786**	0.007	**0.786**	0.001	**0.786**	0.050
GaR^{MOM}	**0.786**	0.003	**0.786**	0.003	**0.786**	0.004	**0.786**	0.004	**0.455**	0.009
GaR^{VXO}	**0.786**	**0.864**	**0.860**	**0.462**	**0.860**	**0.68**	**0.547**	**0.709**	**0.312**	**0.119**
$GaR^{CSPREAD}$	**0.455**	**0.875**	**0.455**	**0.860**	**0.455**	**0.856**	**0.455**	**0.856**	**0.208**	**0.616**
GaR^{TERM}	**0.455**	0.015	**0.455**	0.015	**0.455**	0.015	**0.455**	0.015	**0.786**	0.004
GaR^{TED}	**0.312**	**0.328**	**0.312**	**0.327**	**0.312**	**0.320**	**0.312**	**0.315**	**0.312**	**0.324**
GaR^{ADS}	**0.860**	**0.716**	**0.547**	**0.529**	**0.547**	**0.835**	**0.208**	**0.569**	**0.455**	**0.372**

Note: This table shows the following two interval tests for different combined GaR models: Kupiec's (1995) unconditional coverage test (UC), where the null hypothesis is that the proportion of exceedances is equal to the quantile (non-rejection of the null is preferred); and the dynamic quantile test (DQ) of Engle and Manganelli (2004), where the null hypothesis is that the exceedance indicator is an i.i.d. process (non-rejection of the null is preferred). Bold values indicate that model passes the test with a 10% level of probability.

Table 3C.3: EN-Q out-of-sample forecast accuracy based on coverage tests

	$h_d = 0$		$h_d = 10$		$h_d = 20$		$h_d = 40$		$h_d = 60$	
	UC	DQ	UC	DQ	UC	DQ	UC	DQ	UC	DQ
Panel A. Before COVID-19 (2007Q1 to 2019Q4)										
$GaR^{ISPREAD}$	**0.717**	**0.488**	**0.717**	**0.464**	**0.717**	**0.488**	**0.926**	**0.216**	**0.717**	**0.481**
GaR^{EEFR}	**0.926**	0.099	**0.565**	**0.147**	**0.926**	0.002	**0.926**	**0.124**	**0.926**	0.073
GaR^{RET}	**0.717**	0.007	**0.107**	0.000	**0.427**	0.000	**0.717**	0.002	**0.226**	0.010
GaR^{SMB}	**0.565**	0.071	**0.565**	0.064	**0.926**	**0.131**	**0.717**	0.012	**0.926**	0.021
GaR^{HML}	**0.107**	0.000	**0.717**	0.032	**0.926**	0.032	**0.427**	0.003	**0.427**	0.017
GaR^{MOM}	**0.565**	0.001	**0.273**	**0.648**	**0.107**	0.000	**0.427**	0.007	**0.427**	**0.134**
GaR^{VXO}	**0.427**	**0.656**	**0.427**	**0.645**	**0.226**	**0.358**	**0.427**	**0.583**	**0.926**	**0.922**
$GaR^{CSPREAD}$	**0.717**	**0.856**	**0.717**	**0.879**	**0.717**	**0.855**	**0.717**	**0.856**	**0.565**	**0.900**
GaR^{TERM}	**0.926**	**0.244**	**0.565**	**0.779**	**0.565**	**0.783**	**0.565**	**0.783**	**0.565**	**0.780**
GaR^{TED}	**0.107**	**0.330**	0.046	**0.235**	**0.107**	**0.329**	0.018	0.068	**0.107**	**0.521**
GaR^{ADS}	**0.565**	**0.741**	**0.926**	**0.678**	**0.565**	**0.573**	0.019	**0.286**	**0.565**	**0.889**
Panel B. Including COVID-19 (2007Q1 to 2020Q4)										
$GaR^{ISPREAD}$	**0.312**	**0.145**	**0.312**	**0.144**	**0.160**	0.028	**0.312**	0.007	**0.160**	0.015
GaR^{EEFR}	**0.547**	0.085	**0.86**	**0.313**	**0.547**	0.001	**0.547**	0.079	**0.547**	0.094
GaR^{RET}	**0.312**	0.000	0.031	0.000	**0.160**	0.000	**0.312**	0.003	0.074	0.001
GaR^{SMB}	**0.86**	0.011	**0.547**	0.000	**0.547**	0.038	**0.312**	0.002	**0.547**	0.016
GaR^{HML}	0.031	0.000	**0.160**	0.000	**0.547**	0.069	0.074	0.000	**0.160**	0.011
GaR^{MOM}	**0.86**	0.000	**0.860**	0.002	0.012	0.000	**0.160**	0.001	**0.160**	0.080
GaR^{VXO}	**0.312**	**0.498**	**0.160**	**0.111**	0.074	0.056	**0.160**	**0.113**	**0.547**	**0.458**
$GaR^{CSPREAD}$	**0.312**	**0.402**	**0.312**	**0.389**	**0.312**	**0.420**	**0.312**	**0.384**	**0.860**	**0.426**
GaR^{TERM}	**0.312**	0.014	**0.547**	**0.129**	**0.547**	0.088	**0.547**	0.074	**0.547**	0.072
GaR^{TED}	0.031	0.039	0.012	0.020	0.031	0.040	0.004	0.003	0.031	0.082
GaR^{ADS}	**0.786**	**0.921**	**0.547**	**0.551**	**0.547**	0.022	**0.208**	**0.432**	**0.547**	**0.776**

Note: This table shows the following two interval tests for different combined GaR models: Kupiec's (1995) unconditional coverage test (UC), where the null hypothesis is that the proportion of exceedances is equal to the quantile (non-rejection of the null is preferred); and the dynamic quantile test (DQ) of Engle and Manganelli (2004), where the null hypothesis is that the exceedance indicator is an i.i.d. process (non-rejection of the null is preferred). Bold values indicate that model passes the test with a 10% level of probability.

Table 3C.4: LASSO-PCA-Q out-of-sample forecast accuracy based on coverage tests

	$h_d = 0$		$h_d = 10$		$h_d = 20$		$h_d = 40$		$h_d = 60$	
	UC	DQ	UC	DQ	UC	DQ	UC	DQ	UC	DQ
Panel A. Before COVID-19 (2007Q1 to 2019Q4)										
$GaR^{ISPREAD}$	**0.926**	**0.226**	**0.717**	**0.227**	**0.926**	**0.16**	**0.926**	0.069	**0.565**	0.050
GaR^{EEFR}	**0.565**	**0.394**	**0.926**	**0.110**	**0.926**	0.025	**0.926**	0.022	**0.717**	0.029
GaR^{RET}	**0.107**	0.050	**0.717**	**0.364**	**0.926**	**0.905**	0.006	0.000	0.018	0.007
GaR^{SMB}	**0.427**	**0.154**	**0.717**	**0.239**	**0.926**	**0.279**	**0.717**	**0.435**	**0.565**	**0.089**
GaR^{HML}	**0.107**	**0.123**	**0.427**	0.009	**0.427**	**0.133**	**0.226**	0.008	**0.427**	**0.336**
GaR^{MOM}	**0.226**	0.084	**0.926**	**0.884**	**0.427**	**0.626**	**0.926**	0.096	0.046	0.006
GaR^{VXO}	**0.107**	**0.481**	**0.226**	**0.570**	**0.226**	**0.382**	**0.107**	**0.189**	**0.717**	**0.711**
$GaR^{CSPREAD}$	**0.717**	**0.146**	**0.717**	**0.148**	**0.926**	**0.923**	**0.926**	**0.925**	**0.565**	**0.929**
GaR^{TERM}	**0.273**	0.003	**0.273**	0.003	**0.926**	**0.200**	**0.565**	0.079	**0.273**	**0.678**
GaR^{TED}	**0.427**	**0.469**	**0.226**	**0.180**	**0.226**	**0.180**	**0.107**	**0.185**	**0.107**	**0.450**
GaR^{ADS}	**0.226**	0.043	**0.427**	0.100	**0.226**	**0.085**	**0.226**	0.014	**0.226**	**0.229**
Panel B. Including COVID-19 (2007Q1 to 2020Q4)										
$GaR^{ISPREAD}$	**0.312**	0.004	**0.160**	0.004	**0.312**	0.001	**0.312**	0.001	**0.547**	0.001
GaR^{EEFR}	**0.547**	0.009	**0.312**	0.002	**0.312**	0.001	**0.312**	0.000	**0.160**	0.002
GaR^{RET}	0.031	0.001	**0.312**	0.046	**0.312**	0.035	0.000	0.000	0.004	0.007
GaR^{SMB}	**0.160**	0.009	**0.160**	0.007	**0.312**	0.028	**0.160**	0.028	**0.547**	0.000
GaR^{HML}	0.031	0.082	0.074	0.000	0.074	0.005	0.031	0.003	0.074	0.041
GaR^{MOM}	0.031	0.038	**0.312**	0.031	0.074	**0.136**	**0.547**	0.037	0.004	0.000
GaR^{VXO}	0.031	0.066	0.074	0.163	0.074	0.074	0.031	0.023	**0.312**	**0.372**
$GaR^{CSPREAD}$	**0.312**	**0.436**	**0.312**	**0.566**	**0.547**	**0.925**	**0.547**	**0.928**	**0.860**	**0.954**
GaR^{TERM}	**0.860**	0.000	**0.860**	0.000	**0.312**	0.006	**0.547**	0.001	**0.860**	0.014
GaR^{TED}	0.074	0.018	0.031	0.002	0.031	0.001	0.012	0.001	0.012	0.015
GaR^{ADS}	0.074	0.001	**0.312**	0.095	0.074	0.023	**0.160**	0.021	0.031	0.004

Note: This table shows the following two interval tests for different combined GaR models: Kupiec's (1995) unconditional coverage test (UC), where the null hypothesis is that the proportion of exceedances is equal to the quantile (non-rejection of the null is preferred); and the dynamic quantile test (DQ) of Engle and Manganelli (2004), where the null hypothesis is that the exceedance indicator is an i.i.d. process (non-rejection of the null is preferred). Bold values indicate that model passes the test with a 10% level of probability.

Table 3C.5: EN-PCA-Q out-of-sample forecast accuracy based on coverage tests

	$h_d = 0$		$h_d = 10$		$h_d = 20$		$h_d = 40$		$h_d = 60$	
	UC	DQ	UC	DQ	UC	DQ	UC	DQ	UC	DQ
Panel A. Before COVID-19 (2007Q1 to 2019Q4)										
Panel A. Before COVID-19 (2007Q1 to 2019Q4)										
$GaR^{ISPREAD}$	**0.717**	**0.422**	**0.717**	**0.256**	**0.926**	**0.159**	**0.926**	0.061	**0.565**	0.054
GaR^{EEFR}	**0.565**	**0.769**	**0.427**	0.060	**0.926**	**0.114**	**0.427**	**0.455**	**0.427**	**0.589**
GaR^{RET}	**0.427**	0.042	**0.427**	**0.507**	**0.226**	0.061	0.006	0.000	0.006	0.002
GaR^{SMB}	**0.427**	**0.607**	0.046	0.001	**0.226**	0.035	**0.226**	**0.219**	**0.926**	0.009
GaR^{HML}	**0.107**	**0.115**	**0.717**	**0.333**	**0.926**	**0.253**	**0.427**	**0.120**	**0.717**	**0.155**
GaR^{MOM}	**0.226**	0.083	**0.717**	0.092	**0.226**	**0.716**	**0.427**	0.003	**0.226**	0.021
GaR^{VXO}	**0.226**	**0.614**	**0.107**	**0.188**	**0.226**	**0.383**	**0.107**	**0.337**	**0.427**	**0.725**
$GaR^{CSPREAD}$	**0.717**	**0.147**	**0.717**	**0.148**	**0.926**	**0.919**	**0.926**	**0.925**	**0.565**	**0.930**
GaR^{TERM}	**0.565**	0.062	**0.273**	0.003	**0.926**	**0.198**	**0.565**	0.074	**0.273**	**0.680**
GaR^{TED}	**0.427**	**0.469**	**0.226**	**0.180**	**0.226**	**0.180**	**0.107**	**0.185**	**0.107**	**0.451**
GaR^{ADS}	**0.107**	0.031	**0.226**	0.096	**0.226**	0.006	**0.226**	0.008	**0.226**	**0.390**
Panel B. Including COVID-19 (2007Q1 to 2020Q4)										
$GaR^{ISPREAD}$	**0.160**	0.010	**0.160**	0.005	**0.312**	0.001	**0.312**	0.001	**0.547**	0.001
GaR^{EEFR}	**0.547**	0.026	0.074	0.002	**0.312**	0.003	0.074	0.011	0.074	0.018
GaR^{RET}	**0.160**	0.005	0.074	0.002	0.031	0.000	0.000	0.000	0.001	0.000
GaR^{SMB}	**0.160**	**0.260**	0.004	0.000	0.031	0.000	0.031	0.009	**0.312**	0.000
GaR^{HML}	0.012	0.001	**0.160**	0.003	**0.312**	0.049	0.074	0.014	**0.160**	0.012
GaR^{MOM}	0.031	**0.254**	**0.160**	0.003	0.031	0.032	**0.160**	0.009	0.031	0.000
GaR^{VXO}	0.031	0.074	0.012	0.004	0.031	0.020	0.031	0.053	**0.160**	**0.388**
$GaR^{CSPREAD}$	**0.160**	0.053	**0.160**	**0.107**	**0.312**	**0.407**	**0.547**	**0.923**	**0.860**	**0.953**
GaR^{TERM}	**0.547**	0.001	**0.860**	0.000	**0.312**	0.003	**0.547**	0.001	**0.860**	0.014
GaR^{TED}	0.074	0.018	0.031	0.002	0.031	0.001	0.012	0.001	0.012	0.016
GaR^{ADS}	0.074	0.029	0.074	0.006	0.074	0.001	0.074	0.003	0.031	**0.109**

Note: This table shows the following two interval tests for different combined GaR models: Kupiec's (1995) unconditional coverage test (UC), where the null hypothesis is that the proportion of exceedances is equal to the quantile (non-rejection of the null is preferred); and the dynamic quantile test (DQ) of Engle and Manganelli (2004), where the null hypothesis is that the exceedance indicator is an i.i.d. process (non-rejection of the null is preferred). Bold values indicate that model passes the test with a 10% level of probability.